

## Supporting Information for

### Nickel Sequestration by the Host-Defense Protein Human Calprotectin

Toshiki G. Nakashige,<sup>1,#</sup> Emily M. Zygiel,<sup>1,#</sup> Catherine L. Drennan,<sup>1,2,3,\*</sup> and Elizabeth M. Nolan<sup>1,\*</sup>

<sup>1</sup>Department of Chemistry, <sup>2</sup>Department of Biology, and <sup>3</sup>Howard Hughes Medical Institute, Massachusetts Institute of Technology, Cambridge, MA 02139, USA

#Co-first author

\*Corresponding author: [cdrennan@mit.edu](mailto:cdrennan@mit.edu) and [lnolan@mit.edu](mailto:lnolan@mit.edu)

Phone: 617-452-2495

Fax: 617-324-0505

This Supporting Information contains:

<b>Experimental Section</b>	S4
Materials and General Methods	S4
Preparation of Biotinylated Calprotectin Variants	S5
Liquid Chromatography Mass Spectrometry (LC-MS)	S5
Inductively Coupled Plasma-Mass Spectrometry (ICP-MS)	S6
Analytical Size-Exclusion Chromatography (SEC)	S6
Circular Dichroism (CD) Spectrometry	S7
Crystallization Ni(II)- and Ca(II)-Bound CP-Ser	S7
Data Collection, Processing, and Structure Determination	S8
Metal Substitution Assay	S9
Preparation of Metal-Depleted Chemically Defined Medium (dCDM)	S10
Antimicrobial Activity Assay	S11
Preparation of Metal-Depleted Chemically Defined Urea Broth (dCDMU)	S12
Urease Assay	S13
Phenol-Hypochlorite Assay to Detect Ammonium in Cell Lysate	S14
Nickel Uptake Assay	S16
<b>Supporting Discussion on the Metal Ion Occupancy of the EF-Hand Domains</b>	S17
<b>Supporting Tables and Figures</b>	S18
<b>Table S1.</b> Nomenclature for Human Calprotectin Variants	S18
<b>Table S2.</b> Crystallographic Data Collection and Refinement Statistics	S19
<b>Table S3.</b> Average Ni–Ligand Bond Distances at the His <sub>6</sub> Motif (Site 2)	S20
<b>Table S4.</b> Average Ligand–Ni(II)–Ligand Bond Angles at the His <sub>6</sub> Motif (Site 2)	S20
<b>Table S5.</b> Average Ni–Ligand Bond Distances at the His <sub>3</sub> Asp Motif (Site 1)	S20
<b>Table S6.</b> Average Ligand–Ni(II)–Ligand Bond Angles at the His <sub>3</sub> Asp Motif (Site 1)	S20
<b>Table S7.</b> Components of Metal-Depleted Chemically Defined Medium (dCDM)	S21
<b>Table S8.</b> Inductively Coupled Plasma-Mass Spectrometry (ICP-MS) Analysis of dCDM	S22

<b>Table S9.</b> Bacterial Strains Employed in this Study	S22
<b>Table S10.</b> CFU/mL Quantification of <i>Staphylococcus aureus</i> and <i>Klebsiella pneumoniae</i> Suspensions in the Urease Activity Assays	S23
<b>Table S11.</b> Ni(II) Coordination Motifs in the Protein Data Bank	S24
<b>Table S12.</b> Stability Constants of Small-Molecule Imidazole-Containing Ligands	S25
<b>Figure S1.</b> Composite Omit Maps Associated with the EF-Hand Domains	S26
<b>Figure S2.</b> Structural Alignment of Ni(II)- and Ca(II)-bound CP-Ser and Mn(II)-, Ca(II)-, and Na(I)-bound CP-Ser	S27
<b>Figure S3.</b> ICP-MS Analysis of Size-Exclusion Chromatography (SEC) Eluent Fractions	S28
<b>Figure S4.</b> Preparation of B- $\Delta$ His <sub>3</sub> Asp	S29
<b>Figure S5.</b> Characterization of B- $\Delta$ His <sub>3</sub> Asp	S30
<b>Figure S6.</b> SDS-PAGE of B- $\Delta$ His <sub>3</sub> Asp with Streptavidin Resin Treatment	S31
<b>Figure S7.</b> Schematic Cartoon of the Metal Substitution Assay	S31
<b>Figure S8.</b> Antimicrobial Activity Assay with Metal Preincubation	S32
<b>Figure S9.</b> Nickel Uptake and Urease Activity Assay with <i>S. aureus</i> ATCC 29213 and <i>S. aureus</i> M2	S33
<b>Figure S10.</b> Antimicrobial Activity Assay in dCDM with 2 mM Ca(II)	S34
<b>Figure S11.</b> Schematic Cartoon of the Urease Activity Assay	S35
<b>Figure S12.</b> Urease Activity Assay with <i>K. pneumoniae</i> ATCC 13883	S36
<b>Supporting References</b>	S37

## Experimental Section

**Materials and General Methods.** All solvents and chemicals were obtained from commercial suppliers and used as received. All aqueous solutions and media were prepared using Milli-Q water (18.2 M $\Omega$ ·cm, 0.22- $\mu$ m filter). Buffers were prepared with Ultrol grade HEPES (Calbiochem), TraceSELECT NaCl (Sigma), and TraceSELECT NaOH (Sigma) in either acid-washed volumetric glassware or polypropylene containers, using disposable plastic spatulas or polypropylene pipettes. Stock solutions of metal ions were prepared in acid-washed volumetric glassware by dissolving 99.99% CaCl<sub>2</sub> (1.0 M), 99.999% MnCl<sub>2</sub> (100 mM), 99.997% (NH<sub>4</sub>)<sub>2</sub>Fe(SO<sub>4</sub>)<sub>2</sub>·6H<sub>2</sub>O (100 mM), 99.99% NiCl<sub>2</sub> (1.0 M), 99.99% NiSO<sub>4</sub> (1.0 M), and 99.999% anhydrous ZnCl<sub>2</sub> (1.0 M) (Sigma) into water and transferring the solutions to polypropylene containers. The NiCl<sub>2</sub> salt was used for crystallographic and biochemical experiments, and the NiSO<sub>4</sub> salt was used for the microbiology experiments. Working stock solutions of metal ions for experiments were prepared by serial dilution immediately before use. For microbiology experiments, tryptic soy broth (TSB, BD) was autoclaved and stored at room temperature. The preparation of a metal-depleted chemically defined medium (dCDM) is described below. To minimize metal contamination, the highest purity available reagents were used to prepare the medium. All salts were trace metals basis grade (Sigma). The amino acids, D-glucose, thiamine HCl, and nicotinic acid were all molecular biology grade (Sigma). All bacterial strains (Table S13) were stored as glycerol stocks in TSB at -80 °C. CP protein variants were overexpressed and purified as described elsewhere.<sup>1,2</sup> We employed CP-Ser and metal-binding site variants based on this protein (Table S1). CP-Ser is the heterooligomer of S100A8(C3S) and S100A9(C42S), has comparable antimicrobial activity to native CP,<sup>1</sup> and lacks the native Cys residues that could cause experimental complications due to formation of disulfide bonds. Protein stocks were thawed only once immediately prior to use. Protein concentrations are reported for the  $\alpha\beta$  heterodimer and were determined by A<sub>280</sub> using the extinction coefficient of the CP heterodimer ( $\epsilon_{280} = 18,450 \text{ M}^{-1} \text{ cm}^{-1}$ ) obtained from the online ExPASy ProtParam tool.



**Preparation of Biotinylated Calprotectin Variants.** The biotinylated CP variant biotin- $\Delta$ His<sub>3</sub>Asp (B- $\Delta$ His<sub>3</sub>Asp) was prepared by conjugating biotin polyethyleneoxide iodoacetamide (BPEOIA, Sigma) to the free Cys3 thiol of the S100A9 subunit of CP(C42S)  $\Delta$ His<sub>3</sub>Asp (the heterooligomer of S100A8(C42S)(H83A)(H87A) and S100A9(H20A)(D30A)), respectively. The preparation and overexpression of these S100 subunits were described previously.<sup>1</sup>

CP(C42S)  $\Delta$ His<sub>3</sub>Asp was prepared following the standard CP purification protocol.<sup>1</sup> This procedure includes anion-exchange chromatography (MonoQ 10/100 GL column, GE Life Sciences) and preparative size-exclusion chromatography (SEC) (HiLoad 26/600 S75 pg column, GE Life Sciences) conducted at 4 °C. The running buffers employed during the purification contained 5 mM 1,4-dithiothreitol (DTT, G Biosciences). Following SEC (20 mM HEPES, 100 mM NaCl, 5 mM DTT, pH 8.0), the protein-containing fractions were combined and were buffer exchanged into 20 mM HEPES, 100 mM NaCl, 50  $\mu$ M tris(2-carboxyethyl)phosphine (TCEP, Alfa Aesar), pH 7.5 using a 15-mL 10K MWCO Amicon spin concentrator. To a solution of 50  $\mu$ M protein (diluted in buffer at scales ranging between 40 and 70 mg protein in volumes of 30–60 mL), 150  $\mu$ M BPEOIA was added from a freshly prepared  $\approx$ 15 mM stock solution dissolved in the same buffer. The mixture was incubated at 25 °C on a rocking platform for 1.5 h. Another 150  $\mu$ M BPEOIA was added to the reaction, and the mixture was incubated for another 1.5 h at 25 °C. The reaction was quenched by adding 5 mM  $\beta$ -mercaptoethanol (BME, Calbiochem) and incubating for 5 min. Excess BPEOIA was removed by dialysis against 4 L of 20 mM HEPES, 100 mM NaCl, pH 8.0 overnight at 4 °C. The resulting protein was purified by preparative SEC (20 mM HEPES, 100 mM NaCl, pH 8.0) at 4 °C. The eluent fractions containing protein were combined and dialyzed against 20 mM HEPES, 100 mM NaCl, pH 8.0 containing 10 g Chelex resin (Bio-Rad Laboratories) overnight at 4 °C. The protein was concentrated to 500  $\mu$ M, flash frozen in liquid nitrogen, and stored in 50- $\mu$ L aliquots at 80 °C. The biotinylation was confirmed by mass spectrometry.

**Liquid Chromatography Mass Spectrometry (LC-MS).** Mass spectrometric analysis was conducted using an Agilent Poroshell 300SB-C18 column on an Agilent 1260 LC system

with an Agilent Jetstream ESI. Protein samples (1–3  $\mu\text{M}$ ) were prepared by diluting each protein sample in Milli-Q water, and 5  $\mu\text{L}$  was injected onto the column. The protein was eluted using a denaturing protocol with a solvent gradient of 60–85% B over 13 min at 0.2 mL/min. Solvent A was 0.1% formic acid in water, and solvent B was 0.1% formic acid in acetonitrile. The polypeptide masses were determined using the maximum entropy deconvolution algorithm provided in the Agilent MassHunter BioConfirm software.

**Inductively Coupled Plasma-Mass Spectrometry (ICP-MS).** Metal analysis was conducted using an Agilent 7900 ICP-MS system in helium mode outfitted with an integrated autosampler housed in the Center for Environmental Health Sciences (CEHS) Bioanalytical Core Facility at MIT. The instrument was calibrated using standards prepared by serial dilution of the Agilent Environmental Calibration Standard solution. The concentrations of Mg, Ca, Mn, Fe, Co, Ni, Cu, and Zn were quantified, and terbium (1 ppb Tb; Agilent) was used as an internal standard. Samples were prepared in 15-mL Falcon tubes, and 2-mL samples were transferred to ICP-MS polypropylene vials (Agilent) and analyzed. Sample preparation for each experiment is described below.

For metal analysis of bacterial suspensions, bacteria diluted into solutions of 3%  $\text{HNO}_3$  were liquefied using a Milestone UltraWAVE digestion system housed in the CEHS Core Facility at MIT. A standard microwave protocol (15 min ramp to 200  $^\circ\text{C}$  at 1,500 W power; 10 min ramp to 220  $^\circ\text{C}$  at 1,500 W power) was used for the acid digestion.

**Analytical Size-Exclusion Chromatography (SEC).** An ÄKTA purifier with a Superdex 75 10/300 GL column (GE Healthcare Life Sciences) housed at 4  $^\circ\text{C}$  was used to perform analytical SEC experiments. The calibration of the column using a low-molecular-weight calibration kit (GE Healthcare Life Sciences), and the SEC elution protocol were described previously.<sup>1</sup> Protein solutions were buffer exchanged into 75 mM HEPES, 100 mM NaCl, pH 7.0 buffer prior to running on the SEC column. For biochemical characterization of B- $\Delta\text{His}_3\text{Asp}$ , protein samples (20  $\mu\text{M}$ , 300  $\mu\text{L}$ ) were loaded into a 100- $\mu\text{L}$  loop, and to ensure that the total volume in the loop was transferred to the column, a 500- $\mu\text{L}$  volume was injected. The protein

was eluted over 1 column volume of running buffer (75 mM HEPES, 100 mM NaCl, pH 7.0). For samples in the presence of Ca(II), 2 mM Ca(II) was included in the running buffer.

To determine the Ni(II)-binding stoichiometry of CP, 300  $\mu$ M protein samples in the absence and presence of 5 equiv Ni(II) were injected onto the loop and analyzed following the SEC elution protocol described above. Eluent fractions (0.5 mL) were collected during the SEC run. The protein concentration in the fractions was measured by  $A_{280}$  using the extinction coefficient of CP  $\alpha\beta$  heterodimer ( $\epsilon_{280} = 18,450 \text{ M}^{-1}\text{cm}^{-1}$ ) determined using the online ExPASy ProtParam tool. To measure the Ni content in the fractions, a 400- $\mu$ L aliquot of each fraction was diluted 1:5 into 1.6 mL of 3% nitric acid ( $\text{HNO}_3$ ), and 100  $\mu$ L of concentrated  $\text{HNO}_3$  and 40  $\mu$ L of 50 ppb Tb were added. The resulting mixture was analyzed by ICP-MS (*vide supra*), and the reported Ni concentrations were corrected for the 1:5 sample dilution.

**Circular Dichroism (CD) Spectroscopy.** CD spectra were collected using an Aviv Model 420 Circular Dichroism (CD) spectrometer with a circulating water bath maintained at 25  $^{\circ}$ C. A thin-walled Hellma quartz cuvette was washed with 20%  $\text{HNO}_3$  and Milli-Q water before and in between each experiment. Protein samples (10  $\mu$ M, 300  $\mu$ L) were prepared in 1.0 mM Tris-HCl, pH 7.5 buffer. For samples with Ca(II), 2 mM Ca(II) was added from a 100-mM stock solution. Spectra were collected from 260 to 195 nm (3 independent scans per wavelength, 3 sec averaging time, 1 nm step).

**Crystallization of Ni(II)- and Ca(II)-bound CP-Ser.** Initial crystallization conditions of Ni(II)-bound CP-Ser were identified by screening using a Phoenix Liquid Handling System (Art Robbins Instrument). Larger crystals were subsequently obtained by optimization of the initial crystallization conditions by sitting-drop vapor diffusion at room temperature employing 24-well crystallization plates (Hampton Research). Solutions (100  $\mu$ L) of 100  $\mu$ M CP-Ser (2.4 mg/mL) were prepared in 75 mM HEPES, 100 mM NaCl, pH 7.0 by buffer exchanging purified protein stocks using 10K MWCO Amicon spin filters (Millipore). Ni(II) (100  $\mu$ M) was added to protein samples from a 100-mM aqueous Ni(II) stock solution prepared from  $\text{NiCl}_2$  and gently mixed by pipetting. Protein sample (1  $\mu$ L) was pipetted to each sitting drop, and precipitant solution (1  $\mu$ L)

that contained 200 mM Li<sub>2</sub>SO<sub>4</sub>, 100 mM Tris, 20% (v/v) PEG 3350, pH 8.0 was added to the droplet. The crystallization sample was allowed to equilibrate against 500 μL of precipitant solution. Protein crystals formed in an orthorhombic *P*2<sub>1</sub>2<sub>1</sub>2<sub>1</sub> space group within 3 to 5 days.

We were unable to obtain crystals suitable for diffraction by co-crystallization in the presence of Ca(II). Therefore, the crystals with Ni(II) were soaked in precipitant solution with excess Ca(II) to obtain Ni(II)- and Ca(II)-bound CP-Ser crystals. Precipitant solution (2 μL) of 200 mM Li<sub>2</sub>SO<sub>4</sub>, 100 mM Tris, 20% (w/v) PEG 3350, 5 mM CaCl<sub>2</sub>, pH 8.0 was added to droplets containing Ni(II)-bound CP-Ser crystals, and the resulting samples were allowed to equilibrate at room temperature for 5 days. The protein crystals were transferred to a cryogenic solution (200 mM Li<sub>2</sub>SO<sub>4</sub>, 100 mM Tris, 30% (w/v) PEG 3350, 10% (w/v) PEG 200, 5 mM CaCl<sub>2</sub>, pH 8.0), allowed to equilibrate for ≈10 s, flash frozen in liquid nitrogen, and stored in a liquid nitrogen dewar.

**Data Collection, Processing, and Structure Determination of Ni(II)- and Ca(II)-Bound CP-Ser.** All data were collected at beamline 24ID-C at the APS using a Pilatus 6M pixel detector at 100 K in 0.25° oscillation steps (Table S2). Native datasets were collected at 0.9792 Å (12,622 eV). Ni anomalous datasets were collected at 1.4831 Å (8,360 eV). Data were processed in HKL2000.<sup>3</sup> Like all other programs used during the structural analysis, HKL2000 is part of the SBCGrid software package.<sup>4</sup> The structure of Mn(II)-bound CP-Ser (protein atoms of chains A and B; PDB: 4XJK)<sup>5</sup> in space group *P*2 was used to solve the structure of Ni(II)-bound CP-Ser in space group *P*2<sub>1</sub>2<sub>1</sub>2<sub>1</sub> by molecular replacement in Phaser.<sup>6</sup> The resulting Ni(II)- and Ca(II)- CP-Ser structure was solved to 2.6-Å resolution with two α<sub>2</sub>β<sub>2</sub> heterotetramers in the asymmetric unit (Table S2). The structures were completed by iterative refinement in PHENIX,<sup>7</sup> employing two-fold non-crystallographic symmetry, and model building in Coot.<sup>8</sup> The Ni anomalous datasets were processed using HKL2000, and anomalous density maps were generated in PHENIX.

Protein residues were adjusted first during model building, and the metals and water molecules were added after several rounds of refinement. Composite omit maps were employed

to validate the structure. The presence and occupancy of Ni(II) ions were determined using the Ni anomalous data. Refinement of the Ni(II) ion at the His<sub>3</sub>Asp motif (site 1) at 100% occupancy resulted in negative difference electron density, and in the final model the Ni(II) ion was refined to 75% occupancy. When the occupancy of Ni(II) was refined, the B-factors were fixed to the average B-factor of the coordinating atoms. Ca(II) and Na(I) ions were added to the structure based on the electron density at the EF-hand domains. Ca(II) ions were modeled at the EF-hand domains where Na(I) ions refined with positive difference electron density and Ca(II) ions refined with no difference electron density. Na(I) ions were modeled at the EF-hand domains where Ca(II) ions refined resulted in negative difference electron density and Na(I) ions refined with no difference electron density. No distance or angle restraints were used in the refinement of the metal sites. No difference in metal speciation was observed between the two heterotetramers in the asymmetric unit. The final model of the Ni(II)- and Ca(II)-bound CP-Ser  $\alpha_2\beta_2$  heterotetramer comprises of residues 1–87 for chain A (93 residues total), residues 5–111 for chain B (114 residues total), residues 1–88 for chain C (93 residues total), and residues 5–112 (114 residues total).

**Metal Substitution Assay.** Protein solutions were buffer exchanged into 75 mM HEPES, 100 mM NaCl, pH 7.0 buffer. Samples (1 mL) with 10  $\mu$ M B- $\Delta$ His<sub>3</sub>Asp were prepared in 75 mM HEPES, 100 mM NaCl, 2 mM CaCl<sub>2</sub>, pH 7.0 in 1.7-mL microcentrifuge tubes. To determine the relative affinities of site 2 for Ni(II) and Zn(II), the two metals were added sequentially to the protein solution. For the addition of the first metal, 10  $\mu$ M M(II) was added from 1.0 mM stock solutions. The samples were allowed to equilibrate for 30 min at room temperature, and the second metal (10  $\mu$ M) was then added. The samples were incubated for 72 h at 37 °C on an inverting platform. Samples with and without protein where only one metal was added were also prepared as controls and incubated for 72 h at 37 °C.

After the 72-h incubation, samples were treated with high capacity streptavidin agarose resin (Pierce, Thermo Scientific). We encountered issues of metal contamination by using commercially available Pierce streptavidin magnetic beads from Thermo Scientific (data not

shown) and therefore utilized the agarose resin. Resin (150  $\mu\text{L}$ ) was washed three times with 500  $\mu\text{L}$  buffer (75 mM HEPES, 100 mM NaCl, pH 7.0) by centrifuging (13,000 rpm, 3 min, 4  $^{\circ}\text{C}$ ), removing the supernatant, and resuspending with fresh buffer. After a final centrifugation step, the buffer supernatant was removed, and 500  $\mu\text{L}$  of the metal/protein sample (called “load”) was added to the resin.

The resin mixture was mixed by inverting and allowed to equilibrate for 30 min on a rocking platform at room temperature to allow binding between B- $\Delta\text{His}_3\text{Asp}$  and the streptavidin resin. The resin was pelleted by centrifugation, and 400  $\mu\text{L}$  of the remaining solution without B- $\Delta\text{His}_3\text{Asp}$  (called “supernatant”) were transferred to 15-mL Falcon tubes with 1.6 mL of 3%  $\text{HNO}_3$ , 100  $\mu\text{L}$  of concentrated  $\text{HNO}_3$ , and 40  $\mu\text{L}$  of 1 ppb Tb for ICP-MS analysis. In addition, ICP-MS samples were prepared from 400  $\mu\text{L}$  of the load samples. The load samples were analyzed to measure the total metal content in the B- $\Delta\text{His}_3\text{Asp}$  samples prior to resin treatment, and the supernatant samples, obtained after pull-down, were analyzed to measure the unbound metal content. The ICP-MS results are corrected for the 1:5 dilution of the sample. Four independent trials were conducted, and the mean metal concentration and SDM are reported ( $n = 4$ ). No protein controls were also prepared, treated with resin as described above, and the resulting supernatants analyzed by ICP-MS. For these controls, the mean metal concentration and SDM are reported ( $n = 2$ ).

**Preparation of Metal-Depleted Chemically Defined Medium (dCDM).** A metal-depleted chemically defined medium (dCDM) was prepared with components listed in Table S7, modified from a previous protocol.<sup>9</sup> For the phenol-hypochlorite assays (*vide infra*), a metal-depleted chemically defined medium lacking ammonium was also prepared with all components listed in Table S7 except for ammonium sulfate. All concentrated stocks were prepared in acid-washed volumetric flasks and sterilized by syringe filtration (0.22  $\mu\text{m}$ ) into sterile 50-mL Falcon tubes. After combining all components in a polypropylene beaker ( $\approx 400$  mL), the pH of the medium was adjusted to 6.8 using 30% NaOH. The final volume of the medium was adjusted to 500 mL, and the solution was filter-sterilized using a 0.22- $\mu\text{m}$  bottle-top filter. The medium was

partitioned into 40-mL aliquots in sterile 50-mL Falcon tubes. We observed inconsistent bacterial growth behavior in dCDM stored at room temperature for more than one week and therefore stored the medium at  $-80\text{ }^{\circ}\text{C}$  in the dark. Aliquots were thawed only once prior to an experiment.

Agar plates with dCDM were prepared by autoclaving 250 mL of 3% (w/v) Bacto agar (BD). The agar solution was allowed to stir at room temperature until cool to touch, and 250 mL of dCDM was slowly added while stirring. Plates were immediately poured in petri dishes using sterile technique. The plates were stored at  $4\text{ }^{\circ}\text{C}$  until use.

**Antimicrobial Activity Assay.** To compare the growth inhibitory activity of B- $\Delta\text{His}_3\text{Asp}$  with that of  $\Delta\text{His}_3\text{Asp}$ , standard antimicrobial activity assays were conducted with these proteins against *E. coli* ATCC 25922 in Tris:TSB +BME  $\pm\text{Ca(II)}$  medium, a 62:38 (v:v) mixture of 20 mM Tris-HCl, 100 mM NaCl, 5 mM BME,  $\pm 3\text{ mM CaCl}_2$ , pH 7.5 and TSB. The  $t = 20\text{ h}$  time point ( $30\text{ }^{\circ}\text{C}$ , 150 rpm) is reported. Three independent trials were conducted with at least two different protein preparations for each variant, and the mean  $\text{OD}_{600}$  values and SEM are reported ( $n = 3$ ). Details of the protocol have been described previously.<sup>1</sup>

For evaluating the effect of Ni(II) preincubation on the antibacterial activity of CP against *E. coli* ATCC 25922 and *S. aureus* ATCC 25923, a 5-mL volume of TSB was inoculated using either bacterial freezer stocks or single colonies selected from agar plates, and incubated at  $37\text{ }^{\circ}\text{C}$  on a rotating wheel. At  $t = 16\text{--}20\text{ h}$ , the overnight cultures were diluted 1:100 and incubated at  $37\text{ }^{\circ}\text{C}$  on a rotating wheel for 2–2.5 h until  $\text{OD}_{600} \approx 0.6$  (mid-log phase). Tris:TSB +BME +Ca(II) was prepared using sterile technique. CP samples were buffer exchanged three times into 20 mM Tris-HCl, 100 mM NaCl, pH 7.5 using pre-sterilized 0.5-mL 10K MWCO Amicon spin concentrators, and  $1.1\times$  concentrated protein stocks (1.1 mg/mL to 68.75  $\mu\text{g/mL}$ ) were prepared in the medium in the absence and presence of 0.9 or 1.9 equiv Ni(II). The  $\text{OD}_{600} \approx 0.6$  bacterial cultures were diluted 1:56, and in a flat-bottom 96-well polystyrene plate (Corning), each well was filled with 10  $\mu\text{L}$  of bacterial culture and 90  $\mu\text{L}$  of protein solution. The plates were sealed

with Parafilm and incubated at 30 °C, 150 rpm. At t = 20 h, the OD<sub>600</sub> values were measured using a BioTek Synergy HT plate reader. The mean OD<sub>600</sub> values and SEM are reported (*n* = 3).

For evaluating the effect of Zn(II) preincubation on the antibacterial activity of CP against *E. coli* ATCC 25922, the above protocol was modified. Instead of preincubation with 0.9 or 1.9 equiv Ni(II), protein samples of CP-Ser, ΔHis<sub>3</sub>Asp, and ΔHis<sub>4</sub> were preincubated with 1.0 or 2.0 equiv Zn(II). The assay was conducted as described above for Ni(II) preincubation, and the mean OD<sub>600</sub> values at t = 20 h (30 °C, 150 rpm) and SEM are reported (*n* = 3).

Antimicrobial activity assays of CP-Ser against *S. aureus* USA300 JE2 and *K. pneumoniae* ATCC 13883 were performed in dCDM supplemented with 2 mM Ca(II). Overnight bacterial cultures were inoculated from single colonies on dCDM agar plates into 5 mL dCDM and incubated at 37 °C, 200 rpm. The overnight cultures were diluted 1:100 into fresh dCDM and allowed to grow to OD<sub>600</sub> ≈ 0.6 at 37 °C, 200 rpm (t ≈ 4–6 h). These mid-log phase cultures were diluted 1:500 into dCDM with 2 mM Ca(II). The Ca(II)-supplemented medium was prepared by adding Ca(II) from a filter-sterilized stock solution of 1.0 M CaCl<sub>2</sub>. CP-Ser was buffer exchanged into sterile phosphate buffer (20 mM NaH<sub>2</sub>PO<sub>4</sub>, 100 mM NaCl, pH 6.8), and 10× protein stocks (10 mg/mL to 625 μg/mL) were prepared in dCDM with 2 mM Ca(II). To each well in a 96-well plate, 10 μL of protein and 90 μL of bacteria were added. Each condition was performed in technical triplicate, and three independent trials were conducted. Plates were tightly covered with plastic wrap to prevent evaporation and incubated at 37 °C, 200 rpm. At t = 20 h, the OD<sub>600</sub> values were measured, and the mean OD<sub>600</sub> values and SEM are reported (*n* = 3).

**Preparation of Metal-Depleted Chemically Defined Urea Broth (dCDMU).** A metal-depleted chemically defined urea broth (dCDMU) was prepared by diluting dCDM 1:30 (v:v) in H<sub>2</sub>O and adding 333 mM urea (molecular biology grade, Sigma) and 26.6 μM phenol red (molecular biology grade, Sigma). For a 250-mL volume of dCDMU, 5.0 g urea was dissolved in ≈100 mL H<sub>2</sub>O. To this solution, 664 μL of 10 mM phenol red sodium salt dissolved in H<sub>2</sub>O and 8.3 mL dCDM were added. After the pH was adjusted to 6.8 with HCl (trace metals basis,



Sigma), the solution was brought to a final volume of 250 mL. The final solution was sterilized by syringe filtration (0.22  $\mu\text{m}$ ) into sterile 50-mL Falcon tubes and stored at  $-80\text{ }^{\circ}\text{C}$  until use.

**Urease Activity Assay.** The effect of CP on bacterial urease activity was evaluated for *Staphylococcus aureus* USA300 JE2, *S. aureus* USA300  $\Delta\text{ureC}$ , *S. aureus* USA300  $\Delta\text{cntA}$ , *S. aureus* ATCC 29213, *S. aureus* M2, and *Klebsiella pneumoniae* ATCC 13883 (Table S13). The *S. aureus* USA300 parent and mutant strains were obtained from the Nebraska Transposon Mutant Library (NTML) Screening Array,<sup>10</sup> and *S. aureus* M2 was generously provided by Professor Amanda Oglesby-Sherrouse (University of Maryland School of Pharmacy).<sup>11,12</sup>

Bacteria were streaked onto dCDM plates and incubated at  $37\text{ }^{\circ}\text{C}$  overnight. A single colony was inoculated into 5 mL dCDM and incubated at  $37\text{ }^{\circ}\text{C}$ , 200 rpm overnight (14–24 h). Protein samples were buffer exchanged three times into phosphate buffer (20 mM  $\text{NaH}_2\text{PO}_4$ , 100 mM NaCl, pH 6.8) using pre-sterilized 0.5-mL 10K MWCO Amicon spin concentrators. Solutions of dCDM were supplemented with  $1\text{ }\mu\text{M}$  Ni(II) in the absence or presence of  $1\text{ }\mu\text{M}$  CP-Ser or  $\Delta\Delta$ . The media with protein were supplemented with  $50\text{ }\mu\text{M}$  Ca(II). A control sample without the addition of Ni(II) or protein was also prepared. The overnight bacterial cultures (8 mL for *S. aureus*, 16 mL for *K. pneumoniae*) were diluted 1:100 into each dCDM sample and incubated at  $37\text{ }^{\circ}\text{C}$ , 200 rpm for 14–18 h (*S. aureus*) or for  $\approx 12$  h (*K. pneumoniae*). After incubation, the  $\text{OD}_{600}$  of each bacterial culture was measured ( $\text{OD}_{600} = 0.9\text{--}2.0$ ), and the bacteria were washed twice (*S. aureus*) or three times (*K. pneumoniae*) by centrifugation (3750 rpm,  $4\text{ }^{\circ}\text{C}$ , 7 min), removal of the supernatant, and re-suspension with 1 mL phosphate buffer (stored at  $4\text{ }^{\circ}\text{C}$ ). In the final wash step, cell pellets were re-suspended in phosphate buffer to a calculated  $\text{OD}_{600}$  value of 30 (final volume 350–500  $\mu\text{L}$ ).

Each  $\text{OD}_{600} = 30$  re-suspension (300  $\mu\text{L}$ ) was added to 1.2 mL of dCDMU. These samples were incubated at  $37\text{ }^{\circ}\text{C}$ , 200 rpm. At different time points, a 200- $\mu\text{L}$  aliquot was transferred to a microcentrifuge tube, and the bacteria were pelleted by centrifugation (3750 rpm,  $4\text{ }^{\circ}\text{C}$ , 7 min). The pH of the supernatant was measured using a Micro Bulb pH probe (Hanna Instruments). Mean pH values at each time point and SDM are reported ( $n = 6$  for *S.*

*aureus* USA300 JE2, *S. aureus* USA300  $\Delta cntA$ , and *K. pneumoniae*;  $n = 3$  for *S. aureus* ATCC 29213 and *S. aureus* M2).

To visualize the color change of the phenol red ( $26.2 \mu\text{M}$ ,  $pK_a = 7.5$  at  $25 \text{ }^\circ\text{C}$ )<sup>13</sup> in the dCDMU mixtures,  $500 \mu\text{L}$  of supernatant for each sample was transferred to 2-mL vials and photographed. The photographs presented are of the 2-h or 4-h time point.

To quantify the colony forming units (CFU/mL) of the bacteria in the urease activity assay,  $100 \mu\text{L}$  of the dCDMU suspension at  $t = 0$  and 4 h (*S. aureus*) or  $t = 0$  and 2 h (*K. pneumoniae*) were transferred to wells in a 96-well plate. The bacterial samples were serially diluted in phosphate buffer. Bacteria were plated on TSB agar plates at  $10^{-6}$ ,  $10^{-7}$ , and  $10^{-8}$  dilutions. Colonies were quantified after incubation at  $37 \text{ }^\circ\text{C}$  for 18 h (*S. aureus*) or 12 h (*K. pneumoniae*). The  $\log(\text{CFU/mL})$  values are presented as mean  $\pm$  SEM ( $n=3$  for *S. aureus* USA300 JE2 and *S. aureus* USA300  $\Delta ureC$ , assay presented in Figure 5A;  $n = 6$  for *S. aureus* USA300 JE2, *S. aureus* USA300  $\Delta cntA$ , assay presented in Figure 5B;  $n = 3$  for *S. aureus* ATCC 29213 and *S. aureus* M2, assay presented in Figure S9;  $n = 6$  for *K. pneumoniae*, assay presented in Figure S12).

**Phenol-Hypochlorite Assay.** The effect of CP on ammonia production by urease in *S. aureus* USA300 JE2 cell lysates was evaluated for by using a phenol-hypochlorite assay modified from a literature protocol.<sup>14</sup> The  $\Delta ureC$  mutant was tested as a negative control because it lacks the  $\alpha$  subunit of urease. Bacteria were streaked on TSB agar plates and incubated at  $37 \text{ }^\circ\text{C}$  overnight. A 5-mL volume of dCDM without ammonium sulfate was inoculated with a single colony and the culture was grown for 14–20 h at  $37 \text{ }^\circ\text{C}$ , 200 rpm. Protein samples were buffer exchanged three times into buffer A ( $20 \text{ mM NaH}_2\text{PO}_4$ ,  $100 \text{ mM NaCl}$ ,  $\text{pH } 6.8$ ) using pre-sterilized  $0.5\text{-mL } 10\text{K MWCO}$  Amicon spin concentrators. Solutions of dCDM without ammonium sulfate ( $8 \text{ mL}$ ) were supplemented with  $0.9 \mu\text{M Ni(II)}$  in the absence or presence of  $1 \mu\text{M CP-Ser}$  or  $\Delta\Delta$ . The media with protein were supplemented with  $50 \mu\text{M Ca(II)}$ . A control sample without the addition of  $\text{Ni(II)}$  or protein was also prepared.

The overnight cultures were diluted 1:100 into each dCDM without ammonium and incubated at 37 °C, 200 rpm for 8 h. After incubation, the OD<sub>600</sub> of each bacterial culture was measured (OD<sub>600</sub> = 0.9–1.5), and the bacteria were washed twice by centrifugation (3750 rpm, 7 min, 4 °C), removal of the supernatant, and re-suspension with 1 mL buffer B (50 mM HEPES, pH 7.5). In the final wash step, cell pellets were re-suspended in buffer B to a calculated OD<sub>600</sub> value of 18 (final volume 400-700 µL). Bacterial suspensions (400 µL) were lysed by adding lysostaphin (74 µg/mL, Sigma-Aldrich) and lysozyme (441 µg/mL, Sigma-Aldrich), and incubating at 37 °C for 45 min on a nutating platform. Insoluble lysate was pelleted by centrifugation (13,000 rpm, 4 °C, 5 min).

To determine total protein concentration in each lysate, the soluble lysate (10 µL) was diluted in 40 µL buffer B and a Bradford assay was performed. Bovine serum albumin (BSA) standards (50 µL) were prepared in buffer B from a 1-mg/mL BSA stock solution in water at measured concentrations ranging from 0.44 to 0.09 mg/mL BSA. Bradford reagent (1mL, Bio-Rad Laboratories) was added to each standard or sample and incubated at room temperature for 10 min. The absorbance of each sample was measured at 595 nm, and the total protein concentration in the soluble lysate was determined using the BSA standard curve.

Ammonia development in the cell lysate was monitored by conducting a phenol-hypochlorite assay adapted from a literature protocol.<sup>14</sup> Soluble lysate (10 µL) was diluted in 40 µL buffer B. Ammonium chloride standards (50 µL) were prepared in buffer B at concentrations ranging from 4.00 mM to 0.10 mM. A 200-µL aliquot of buffer C (50 mM HEPES, 25 mM urea, pH 7.5) was added to each diluted lysate or standard, and the resulting solutions were incubated on a nutating platform for 20 min at 37 °C. To detect the level of ammonia in the resulting samples, 375 µL of reagent A (106 mM phenol, 187 µM sodium nitroprusside in Milli-Q H<sub>2</sub>O, stored in the dark at 4 °C) and 375 µL of reagent B (127 mM sodium hydroxide, 0.84% sodium hypochlorite, prepared in Milli-Q H<sub>2</sub>O and stored in the dark at room temperature) were added and the samples were incubated for an additional 45 min at 37 °C on a nutating platform. The absorbance of each sample was measured at 625 nm.

Absorbance readings from the Bradford and phenol-hypochlorite assays were converted to concentration of protein and ammonium, respectively, using the standard curves. All concentrations were corrected for the 1:5 dilution of the lysate. The data are reported as the mean  $\mu\text{mol}$  ammonia / mg protein to control for any variation of protein content in the lysate of each sample. Reported data are an average of two separate trials performed on different days, each of which included three biological replicates and two technical replicates for each sample. The mean and SDM are reported ( $n = 12$ ).

**Nickel Uptake Assay.** The effect of CP on bacterial Ni content was evaluated for *S. aureus* USA300 JE2, *S. aureus* USA300  $\Delta\text{cntA}$ , *S. aureus* ATCC 29213, *S. aureus* M2, and *K. pneumoniae* ATCC 13883.

Bacteria were incubated in dCDM in the absence and presence of 1  $\mu\text{M}$  Ni(II) and 1  $\mu\text{M}$  protein with 50  $\mu\text{M}$  Ca(II), and bacterial suspensions of  $\text{OD}_{600} = 30$  were washed with phosphate buffer (pH 6.8) and prepared as described above. To determine the metal content in the bacterial re-suspensions, 50  $\mu\text{L}$  (*S. aureus*) or 400  $\mu\text{L}$  (*K. pneumoniae*) of each  $\text{OD}_{600} = 30$  re-suspension was transferred to 1.95 mL (*S. aureus*) or 1.6 mL (*K. pneumoniae*) of 3%  $\text{HNO}_3$  in 15-mL Falcon tubes to final volumes of 2.0 mL. Concentrated  $\text{HNO}_3$  (100  $\mu\text{L}$ ) and Tb internal standard (40  $\mu\text{L}$  of 50 ppb solution) were added to these bacterial suspensions. They were liquefied by microwave digestion, and the resulting solutions were analyzed by ICP-MS. The reported metal content for each sample was calculated for bacterial suspensions at an  $\text{OD}_{600} = 6$  (density of bacteria in urease activity assay). The mean metal content and SDM are reported ( $n = 6$  for *S. aureus* USA300 JE2, *S. aureus* USA300  $\Delta\text{cntA}$ , and *K. pneumoniae*;  $n = 3$  for *S. aureus* ATCC 29213 and *S. aureus* M2).

## Supporting Discussion on the Metal Ion Occupancy of the EF-Hand Domains

The occupancies of Ca(II) and Na(I) in the EF-hand domains of the Ni(II)-, Ca(II), and Na(I)-bound CP-Ser structure (Table 1) differ from the metal speciation at the non-canonical EF-hand domains of the two reported Mn(II)- and Ca(II)-bound CP-Ser structures,<sup>5,15</sup> and likely can be attributed to variable crystallization conditions as well as whether anomalous scattering data were available to help distinguish Ca(II) from Na(I). For the first Mn(II)- and Ca(II)-bound structure of CP-Ser, the amount of Ca(II) employed to obtain crystals and Ca(II) anomalous data were not reported, and the structural refinement included Ca(II) ions or no metal at the non-canonical domains.<sup>15</sup> In our Mn(II)- and Ca(II)-bound CP-Ser structure, the protein was crystallized in the presence of 10 equiv Ca(II) per  $\alpha\beta$  heterodimer.<sup>5</sup> Based on anomalous scattering data that showed Ca(II) in the C-terminal EF-hands only, we modeled Na(I) ions at all four non-canonical EF-hands.<sup>5</sup> In the current structure, Ca(II) was added by soaking Ni(II)-bound CP-Ser crystals in a solution containing  $\approx 2.5$  mM CaCl<sub>2</sub>. It is possible that a greater excess of Ca(II) in the soaked Ni(II)-bound crystals compared to the prior conditions for the Mn(II)- and Ca(II)-bound structure resulted in population of the S100A9 non-canonical EF-hand with Ca(II).

## Supporting Tables and Figures

**Table S1.** Nomenclature of Human Calprotectin Variants

<b>Protein</b>	<b>S100A8 Amino Acid Substitution(s)</b>	<b>S100A9 Amino Acid Substitution (s)</b>
CP	N/A	N/A
CP-Ser	C42S	C3S
CP(C42S) $\Delta$ His <sub>3</sub> Asp <sup>a</sup>	C42S, H83A, H87A	H20A, D30A
B- $\Delta$ His <sub>3</sub> Asp <sup>a</sup>	C42S, H83A, H87A	H20A, D30A
CP-Ser $\Delta$ His <sub>3</sub> Asp <sup>b</sup>	C42S, H83A, H87A	C3S, H20A, D30A
CP-Ser $\Delta$ His <sub>4</sub> <sup>b</sup>	C42S, H17A, H27A	C3S, H91A, H95A
CP-Ser $\Delta\Delta$ <sup>b</sup>	C42S, H17A, H27A, H83A, H87A	C3S, H20A, D30A, H91A, H95A

<sup>a</sup> CP(C42S)  $\Delta$ His<sub>3</sub>Asp is the protein variant employed for the preparation of biotinylated  $\Delta$ His<sub>3</sub>Asp (B- $\Delta$ His<sub>3</sub>Asp). Cys3 of the S100A9 subunit was biotinylated using BPEOIA. <sup>b</sup> The metal-binding-site variants are routinely abbreviated as  $\Delta$ His<sub>3</sub>Asp,  $\Delta$ His<sub>4</sub>, and  $\Delta\Delta$  throughout the text.

**Table S2.** Crystallographic Data Collection and Refinement Statistics

<b>Ni(II)- and Ca(II)-bound CP-Ser</b>		
<b>Data collection</b>		
Wavelength (Å)	0.9792	1.4831 <sup>a</sup>
Space group	<i>P</i> 2 <sub>1</sub> 2 <sub>1</sub> 2 <sub>1</sub>	<i>P</i> 2 <sub>1</sub> 2 <sub>1</sub> 2 <sub>1</sub>
Cell dimensions		
<i>a</i> , <i>b</i> , <i>c</i> (Å)	57.0, 77.6, 222.7	57.0, 77.6, 222.7
$\alpha$ , $\beta$ , $\gamma$ (°)	90, 90, 90	90, 90, 90
Resolution (Å)	45.24–2.60 (2.69–2.60)	50.00–3.60 (3.66–3.60)
No. unique reflections	29660 (2247)	13235 (286)
CC <sub>1/2</sub> <sup>b</sup>	(0.887)	(0.930)
<i>R</i> <sub>sym</sub> <sup>b</sup>	0.159 (0.361)	0.137 (0.302)
<i>R</i> <sub>meas</sub> <sup>b</sup>	0.175 (0.406)	0.154 (0.361)
$\langle I \rangle / \sigma (\langle I \rangle)$ <sup>b</sup>	9.3 (3.0)	7.4 (2.6)
Redundancy <sup>b</sup>	5.5 (4.2)	3.9 (2.2)
Completeness <sup>b</sup>	94.5 (72.2)	64.6 (43.4)
<b>Refinement</b>		
Resolution (Å)		
<i>R</i> <sub>cryst</sub> / <i>R</i> <sub>free</sub>	0.224/0.262	
No. atoms		
Protein	6440	
Ni/Ca/Na	6/10/6	
H <sub>2</sub> O	148	
<i>B</i> -factors (Å <sup>2</sup> )		
Protein	32.39	
Solvent	34.90	
Ni	33.59	
Ca	37.45	
Na	36.55	
R.M.S. deviations		
Bond lengths (Å)	0.001	
Bond angles (°)	0.35	
Rotamer outliers (%)	0.14	
Ramachandran		
Outliers (%)	0.13	
Allowed (%)	2.51	
Favored (%)	97.38	

<sup>a</sup> The Ni anomalous dataset was processed with “Scale Anomalous” in HKL2000. <sup>b</sup> Values in parentheses are for highest-resolution shell.

**Table S3.** Average Ni(II)–Ligand Bond Distances at the His<sub>6</sub> Motif (Site 2) <sup>a</sup>

Ligand	Ni–Ligand Bond Distance (Å)
Nε2, (A8)His17	2.2 (0.1)
Nε2, (A8)His27	2.2 (0.1)
Nε2, (A9)His91	2.3 (0.1)
Nε2, (A9)His95	2.2 (0.1)
Nε2, (A9)His103	2.3 (0.0)
Nε2, (A9)His105	2.4 (0.1)

<sup>a</sup> Average (standard deviation) bond distances of both tetramers in the asymmetric unit are shown.

**Table S4.** Ligand–Ni(II)–Ligand Bond Angles at the His<sub>6</sub> Motif (Site 2) (°) <sup>a</sup>

Ligand	Nε2, His17	Nε2, His27	Nε2, His91	Nε2, His95	Nε2, His103	Nε2, His105
Nε2, His17	N/A	93 (5)	93 (7)	169 (3)	90 (1)	87 (6)
Nε2, His27	–	N/A	91 (5)	89 (4)	96 (4)	172 (4)
Nε2, His91	–	–	N/A	86 (6)	174 (3)	92 (6)
Nε2, His95	–	–	–	N/A	95 (4)	86 (2)
Nε2, His103	–	–	–	–	N/A	84 (1)
Nε2, His105	–	–	–	–	–	N/A

<sup>a</sup> Average (standard deviation) bond angles of both tetramers in the asymmetric unit are shown.

**Table S5.** Ni–Ligand Bond Distances at the His<sub>3</sub>Asp Motif (Site 1) <sup>a</sup>

Ligand	Ni–Ligand Bond Distance (Å)
Nε2, (A8)His83	2.1 (0.1)
Nε2, (A8)His87	2.1 (0.0)
Nε2, (A9)His20	2.1 (0.1)
Oδ1, (A9)Asp30 <sup>b</sup>	1.9 (0.0)
Oδ2, (A9)Asp30 <sup>b</sup>	3.0 (0.1)

<sup>a</sup> Average (standard deviation) bond distances of both tetramers in the asymmetric unit are shown. <sup>b</sup> Asp30 coordinates Ni(II) in a monodentate fashion.

**Table S6.** Ligand–Ni(II)–Ligand Bond Angles at the His<sub>3</sub>Asp Motif (Site 1) (°) <sup>a</sup>

Ligand	Nε2, His83	Nε2, His87	Nε2, His20	Oδ1, Asp30
Nε2, His83	N/A	104 (2)	107 (7)	130 (4)
Nε2, His87	–	N/A	101 (2)	98 (5)
Nε2, His20	–	–	N/A	111 (6)
Oδ1, Asp30	–	–	–	N/A

<sup>a</sup> Average (standard deviation) bond angles of both tetramers in the asymmetric unit are shown.



**Table S7.** Components of Metal-Depleted Chemically Defined Medium (dCDM) <sup>a</sup>

<b>Salt</b>	<b>Stock Concentration (M)</b>	<b>Solvent</b>	<b>Final Concentration (mM)</b>
(NH <sub>4</sub> ) <sub>2</sub> SO <sub>4</sub>	1.00	H <sub>2</sub> O	51.8
KH <sub>2</sub> PO <sub>4</sub>	1.00	H <sub>2</sub> O	9.85
NaH <sub>2</sub> PO <sub>4</sub>	2.25	H <sub>2</sub> O	40.2
CaCl <sub>2</sub>	1.00	H <sub>2</sub> O	0.0337
NaCl	1.00	H <sub>2</sub> O	0.0992
MgSO <sub>4</sub>	0.500	H <sub>2</sub> O	2.05
<b>Amino Acid</b>	<b>Stock Concentration (mM)</b>	<b>Solvent</b>	<b>Final Concentration (mM)</b>
L-Cysteine	100	H <sub>2</sub> O	1.98
L-Aspartic acid	500	0.5 M NaOH	18.0
L-Glutamic acid	500	0.5 M NaOH	16.3
L-Proline	500	H <sub>2</sub> O	20.8
L-Arginine	100	H <sub>2</sub> O	2.07
L-Glycine	500	H <sub>2</sub> O	32.0
L-Histidine	100	H <sub>2</sub> O	3.09
L-Lysine HCl	100	H <sub>2</sub> O	3.29
L-Serine	500	H <sub>2</sub> O	22.8
L-Valine	100	H <sub>2</sub> O	4.10
L-Tyrosine	50	1 M NaOH	0.993
L-Threonine	400	H <sub>2</sub> O	20.1
L-Alanine	500	H <sub>2</sub> O	26.9
L-Isoleucine	100	H <sub>2</sub> O	4.57
L-Leucine	100	H <sub>2</sub> O	4.57
L-Phenylalanine	100	H <sub>2</sub> O	1.21
L-Tryptophan	20	0.2 M NaOH	0.294
L-Methionine	100	H <sub>2</sub> O	1.21
<b>Other</b>	<b>Stock Concentration (mM)</b>	<b>Solvent</b>	<b>Final Concentration (mM)</b>
D-Glucose	500	H <sub>2</sub> O	20.2
Thiamine HCl	10	H <sub>2</sub> O	0.00178
Nicotinic Acid	100	H <sub>2</sub> O	0.0970

<sup>a</sup> This recipe was adapted from a previous medium preparation protocol.<sup>9</sup>

**Table S8.** Inductively Coupled Plasma-Mass Spectrometry (ICP-MS) Analysis of dCDM

Trial		Mg	Ca	Mn	Fe	Co	Ni	Cu	Zn
1	ppb	61500	3090	1.53	9.79	0.16	1.36	2.81	11.4
	μM	2530	77.2	0.0278	0.175	0.0028	0.0232	0.0442	0.174
2	ppb	62200	3230	1.56	10.7	0.16	1.41	2.87	15.5
	μM	2560	80.7	0.0284	0.192	0.0027	0.0240	0.0452	0.237
3	ppb	39600	1160	1.00	9.47	0.12	0.23	0.63	8.38
	μM	1630	29.0	0.018	0.170	0.002	0.004	0.010	0.128
4	ppb	36800	1170	0.89	6.25	0.11	0.28	1.47	6.20
	μM	1510	29.2	0.016	0.112	0.002	0.005	0.023	0.095
5	ppb	39200	1180	0.95	9.56	0.11	0.24	0.68	6.16
	μM	1610	29.4	0.017	0.171	0.002	0.004	0.011	0.094

**Table S9.** Bacterial strains employed in this study

Strain	Source	Comments)
<i>S. aureus</i> USA300 JE2	NTML Collection <sup>10</sup>	Parent strain of NTML collection; community isolate; methicillin-resistant
<i>S. aureus</i> USA300 NE1174	NTML Collection <sup>10</sup>	Transposon mutant; single gene knockout of <i>cntA</i> ; strain deficient in CntA staphylopine-binding protein
<i>S. aureus</i> USA300 NE410	NTML Collection <sup>10</sup>	Transposon mutant; single gene knockout of <i>ureC</i> ; strain deficient in $\alpha$ subunit of urease
<i>S. aureus</i> ATCC 29213	ATCC	Quality control and antimicrobial susceptibility testing strain
<i>S. aureus</i> M2 <sup>11,12</sup>	A. Oglesby-Sherrouse, University of Maryland School of Pharmacy	Clinical isolate; methicillin-resistant
<i>K. pneumoniae</i> ATCC 13883	ATCC	Quality control and antimicrobial susceptibility testing strain

**Table S10.** CFU/mL Quantification of *Staphylococcus aureus* and *Klebsiella pneumoniae* Suspensions in the Urease Activity Assays

Strain	Condition	log(CFU/mL) at 0 h	log(CFU/mL) at 4 h
<i>S. aureus</i> USA300 JE2	-Ni(II)	9.3 ± 0.2	9.7 ± 0.3
	+Ni(II)	9.5 ± 0.2	9.6 ± 0.4
<i>S. aureus</i> USA300 $\Delta$ ureC	-Ni(II)	9.5 ± 0.1	9.7 ± 0.7
<i>S. aureus</i> USA300 JE2	-Ni(II)	9.6 ± 0.0	9.8 ± 0.1
	+Ni(II)	9.5 ± 0.1	9.8 ± 0.1
	CP-Ser +Ni(II)	9.6 ± 0.1	9.8 ± 0.1
<i>S. aureus</i> USA300 $\Delta$ cntA	-Ni(II)	9.6 ± 0.1	9.8 ± 0.0
<i>S. aureus</i> ATCC 29213	-Ni(II)	9.2 ± 0.1	9.7 ± 0.2
	+Ni(II)	9.6 ± 0.1	9.9 ± 0.2
	CP-Ser +Ni(II)	9.5 ± 0.2	9.9 ± 0.1
<i>S. aureus</i> M2	-Ni(II)	9.8 ± 0.2	9.9 ± 0.2
	+Ni(II)	9.9 ± 0.2	9.9 ± 0.2
	CP-Ser +Ni(II)	9.7 ± 0.2	10.0 ± 0.3
<i>K. pneumoniae</i> ATCC 13883	-Ni(II)	9.5 ± 0.0	9.5 ± 0.1
	+Ni(II)	9.3 ± 0.1	9.5 ± 0.1
	CP-Ser +N(II)	9.4 ± 0.1	9.4 ± 0.1

**Table S11.** Coordination Motifs in Select Ni(II) Proteins

Protein (Organism) <sup>a</sup>	Coordination Number	Coordination Sphere	Ligands
NikA ( <i>S. aureus</i> ) <sup>16</sup>	6	N <sub>4</sub> O <sub>2</sub>	2 His <sup>b</sup>
Methyl coenzyme M reductase ( <i>Methanothermobacter margburgensis</i> ) <sup>17</sup>	6	N <sub>4</sub> OS	1 Ni-tetrapyrrole, 1 coenzyme M, 1 Gln
Acireductone dioxygenase ( <i>Klebsiella oxytoca</i> ) <sup>18</sup>	6	N <sub>3</sub> O <sub>3</sub>	3 His, 1 Glu, 2 H <sub>2</sub> O
Glyoxylase I ( <i>Escherichia coli</i> ) <sup>19</sup>	6	N <sub>2</sub> O <sub>4</sub>	2 His, 2 Glu, 2 H <sub>2</sub> O
Urease ( <i>Klebsiella aerogenes</i> ) <sup>20 c</sup>	5, 6	N <sub>2</sub> O <sub>3</sub> , N <sub>2</sub> O <sub>4</sub>	2 His, 2 H <sub>2</sub> O, 1 lysine carbamate; 2 His, 2 H <sub>2</sub> O, 1 Asp, 1 lysine carbamate
UreE ( <i>Helicobacter pylori</i> ) <sup>21</sup>	5	N <sub>5</sub>	5 His
Ni superoxide dismutase ( <i>Streptomyces coelicolor</i> ) <sup>22</sup>	5	N <sub>3</sub> S <sub>2</sub>	1 terminal amine, 1 backbone amide, 1 His, 2 Cys
[NiFe]-hydrogenase ( <i>Desulfovibrio fructosovorans</i> ) <sup>23 d</sup>	5	OS <sub>4</sub>	4 Cys, 1 H <sub>2</sub> O
NikR ( <i>E. coli</i> ) <sup>24</sup>	4	N <sub>3</sub> S	3 His, 1 Cys
Lactate racemase LarA ( <i>Lactobacillus plantarum</i> ) <sup>25 e</sup>	4	CNS <sub>2</sub>	1 His, 1 pyridinium-3-thioamide-5-thiocarboxylic acid mononucleotide
NikM ( <i>Thermoanaerobacter tengcongensis</i> ) <sup>26</sup>	4	N <sub>4</sub>	ATCUN motif derived from Met1 and 2 His

<sup>a</sup> The proteins listed in this table are understood to coordinate Ni(II) in nature. A number of examples of Ni(II)-substituted proteins have been structurally characterized and are not included in this analysis. Proteins that contain Ni as part of a metallocluster are also not included. <sup>b</sup> Two L-His molecules coordinate the metal. <sup>c</sup> Urease has a dinuclear active site, and both coordination spheres are listed. <sup>d</sup> The ligand bridging the Ni and Fe centers of this enzyme depend on the state of the protein. <sup>e</sup> Ni is bound to a niacin-derived pincer ligand.

**Table S12.** Stability Constants of Small-Molecule Imidazole-Containing Ligands<sup>27-29 a</sup>

Ligand	Equilibrium <sup>b</sup>	Ni(II)	Zn(II)
Imidazole	ML <sub>4</sub> /M.L <sup>4</sup>	9.1	9.2
	ML <sub>5</sub> /M.L <sup>5</sup>	10.2	–
	ML <sub>6</sub> /M.L <sup>6</sup>	10.7	–
4-(2-Aminoethyl) imidazole <sup>c</sup>	ML <sub>2</sub> /M.L <sup>2</sup>	12.0	9.8
	ML <sub>3</sub> /M.L <sup>3</sup>	15.3	12.1
4-(2-Methylaminoethyl) imidazole	ML/M.L	5.9	4.8
	ML <sub>3</sub> /M.L <sup>3</sup>	18.2	–
4-(2-Dimethylaminoethyl) imidazole	ML/M.L	3.9	3.4
L-Histidine methyl ester <sup>d</sup>	ML/M.L	6.2	4.5
	ML <sub>2</sub> /M.L <sup>2</sup>	11.1	8.7
	ML <sub>3</sub> /M.L <sup>3</sup>	14.0	–
<i>N,N'</i> -Bis(4-imidazolylmethyl) ethylenediamine	ML/M.L	14.0	10.4
2-(2-Pyridyl)imidazole	ML/M.L	6.4	4.4
	ML <sub>2</sub> /M.L <sup>2</sup>	12.6	8.2
	ML <sub>3</sub> /M.L <sup>3</sup>	17.8	10.7
4-(2-Pyridyl)imidazole	ML/M.L	7.2	5.4
	ML <sub>2</sub> /M.L <sup>2</sup>	14.0	10.2
	ML <sub>3</sub> /M.L <sup>3</sup>	19.8	13.8
1-Ethylimidazole <sup>e</sup>	ML <sub>4</sub> /M.L <sup>4</sup>	9.0	9.3
	ML <sub>5</sub> /M.L <sup>5</sup>	9.8	10.1
	ML <sub>6</sub> /M.L <sup>6</sup>	10.2	–
1-Propylimidazole <sup>e</sup>	ML <sub>4</sub> /M.L <sup>4</sup>	9.2	9.2
	ML <sub>5</sub> /M.L <sup>5</sup>	10.3	10.0
	ML <sub>6</sub> /M.L <sup>6</sup>	11.0	–
1,9-Di-4-imidazolyl-2,5,8-triazanonane	ML/M.L	17.4	13.3
1,11-Di-2-imidazolyl-2,6,10-trizaundecane	ML/M.L	15.0	11.9
1,11-Di-4-imidazolyl-2,6,10-trizaundecane	ML/M.L	14.9	11.8
4-(2-Aminoethyl)imidazole	ML/M.L	6.8	5.20
	ML <sub>2</sub> /M.L <sup>2</sup>	11.9	10.1
	ML <sub>3</sub> /M.L <sup>3</sup>	15.0	–
1,9-Di-4-imidazolyl-2,8-diaza-5-oxanonane	ML/M.L	12.4	9.5

<sup>a</sup> Stability constants were measured at 25 °C with an ionic strength of 0.1 M unless otherwise noted. <sup>b</sup> Equilibria are denoted as ML<sub>x</sub>/M.L<sup>x</sup> for M + xL ⇌ ML<sub>x</sub>. <sup>c</sup> The stability constants were measured at 25 °C with an ionic strength of 0.3 M. <sup>d</sup> The stability constants were measured at 25 °C with an ionic strength of 0.16 M. <sup>e</sup> The stability constants were measured at 25 °C with an ionic strength of 0.5 M.

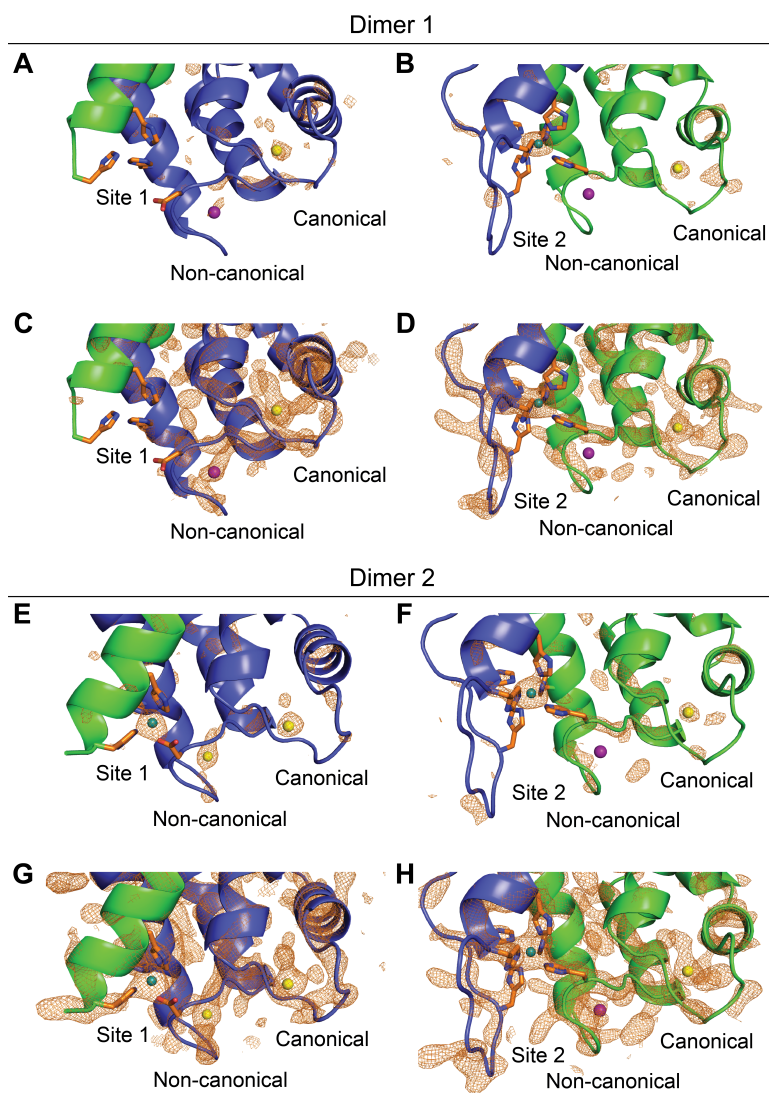


**Figure S1.** Composite omit electron density associated with the EF-hand domains. (**A** and **C**) An omit electron density map (orange mesh) shows no density at His<sub>3</sub>Asp (site 1), consistent with no metal binding; weak density at the non-canonical EF-hand domain, consistent with Na(I) binding; and strong density at the canonical EF-hand domain, consistent with Ca(II) binding. (**B** and **D**) An omit electron density map (orange mesh) shows very strong density at the His<sub>6</sub> site (site 2), consistent with Ni(II) binding; weak density at the non-canonical EF-hand domain, consistent with Na(I) binding; and strong density at the canonical EF-hand domain, consistent with Ca(II) binding. (**E** and **G**) An omit electron density map (orange mesh) shows strong density at His<sub>3</sub>Asp (site 1), consistent with Ni(II) binding and strong density at both EF-hand domains, consistent with Ca(II) binding. (**F** and **H**) An omit electron density map (orange mesh) shows very strong density at the His<sub>6</sub> site (site 2), consistent with Ni(II) binding; weak density at the non-canonical EF-hand site, consistent with Na(I) binding; and strong density at the canonical EF-hand domain, consistent with Ca(II) binding. The S100A9 subunit is blue and S100A8 is green. Ni(II) ions are teal. Ca(II) ions are yellow. Na(I) ions are purple. The *2Fo-Fc* composite omit electron density map is contoured at 5 $\sigma$  (**A**, **B**, **E**, and **F**) or 3 $\sigma$  (**C**, **D**, **G**, and **H**). Ni anomalous difference maps (shown in Figure 1) were used to further differentiate Ni(II) from Ca(II).

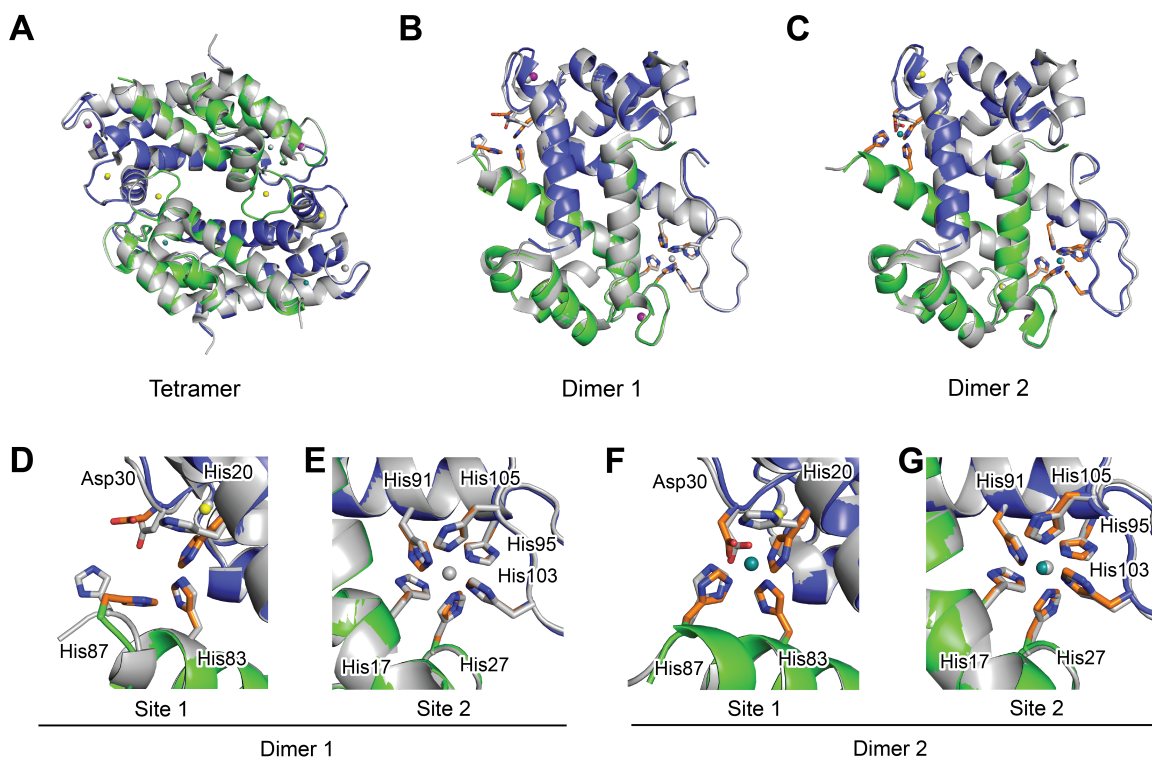


**Figure S2.** Structural alignment of Ni(II)- and Ca(II)-bound CP-Ser and Mn(II)-, Ca(II)-, and Na(I)-bound CP-Ser (PDB: 4XJK).<sup>5</sup> (A) Model of tetramer. (B) Model of dimer 1. (C) Model of dimer 2. (D) Site 1 of dimer 1. (E) Site 2 of dimer 1. (F) Site 1 of dimer 2. (G) Site 2 of dimer 2. The Ni(II)- and Ca(II)-bound structure and the metals associated with this structure are in color. The S100A8 subunit is green. The S100A9 subunit is blue. Ni(II) ions are teal. Ca(II) ions are yellow. Na(I) ions are purple. The Mn(II)-, Ca(II)-, and Na(I) bound structure is in gray.

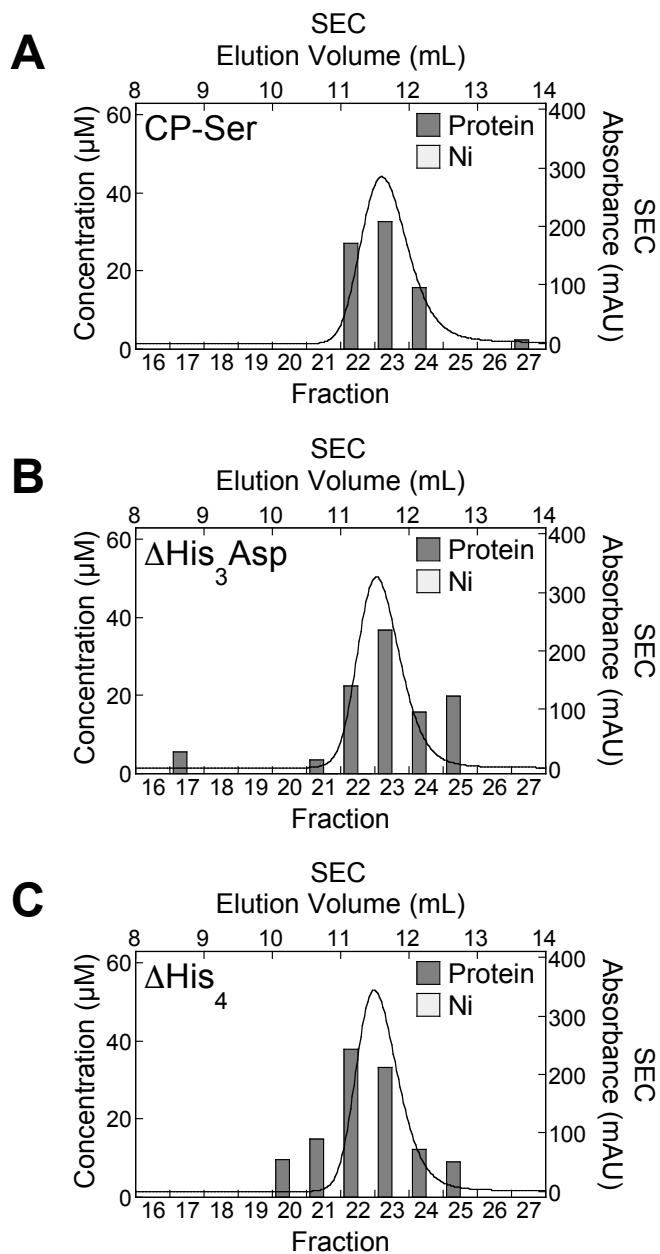


**Figure S3.** Elemental analysis of CP in analytical size-exclusion chromatography (SEC) eluent fractions. Samples of 300 μM **(A)** CP-Ser, **(B)** ΔHis<sub>3</sub>Asp, and **(C)** ΔHis<sub>4</sub> were monitored by analytical SEC in 75 mM HEPES, 100 mM NaCl, pH 7.0. The SEC chromatograms are shown as absorbance (right y-axis) as a function of elution volume (top x-axis). The protein and Ni concentrations (left y-axis) of the eluent fractions (bottom x-axis) were measured by absorbance at 280 nm and by ICP-MS, respectively. Protein concentration is shown as dark gray bars, and the Ni concentration is shown as light gray bars. Data from one representative experiment for each condition are shown.



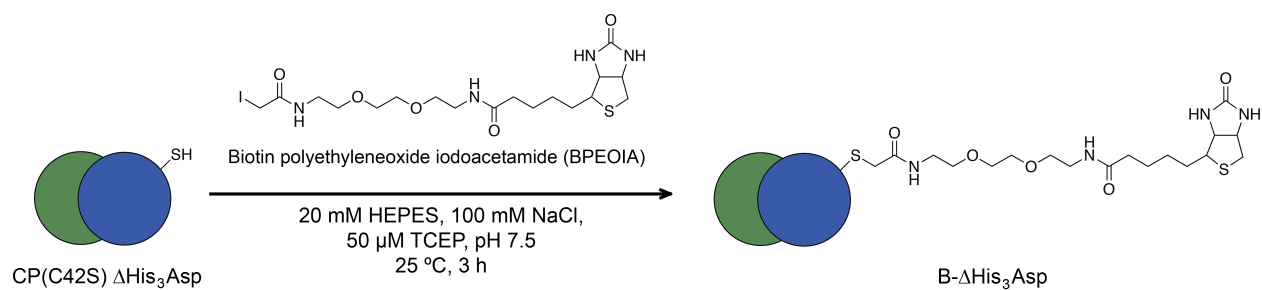


**Figure S4.** Preparation of B- $\Delta$ His<sub>3</sub>Asp. A solution of 50  $\mu$ M CP(C42S)  $\Delta$ His<sub>3</sub>Asp was buffer exchanged into 20 mM HEPES, 100 mM NaCl, 50  $\mu$ M TCEP, pH 7.5, and 150  $\mu$ M biotin polyethyleneoxide iodoacetamide (BPEOIA) from a 1.5-mM stock solution in buffer was added. The mixture was incubated at room temperature on a nutating platform. Another 150  $\mu$ M BPEOIA was added at 1.5 h after the first addition. At t = 3 h, 5 mM BME was added to quench the reaction. B- $\Delta$ His<sub>3</sub>Asp were purified by SEC.

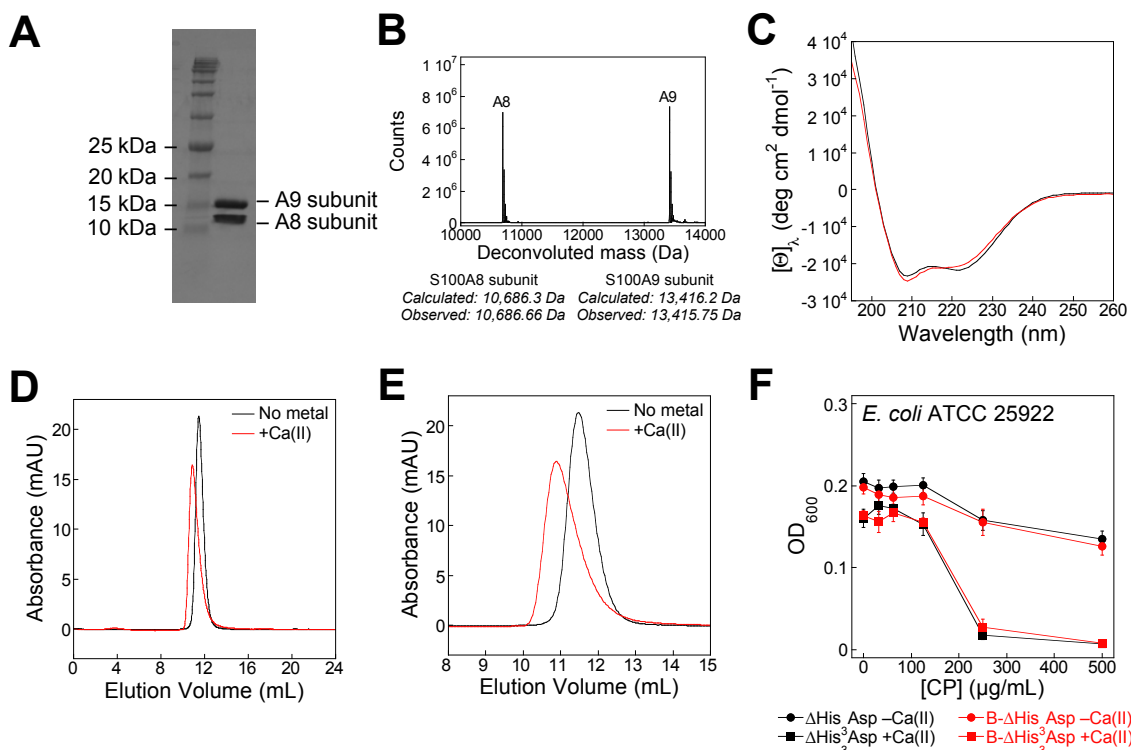


**Figure S5.** Characterization of B- $\Delta$ His<sub>3</sub>Asp. **(A)** SDS-PAGE gel (15% Tris-glycine) of B- $\Delta$ His<sub>3</sub>Asp with the P7704 protein ladder (New England BioLabs). **(B)** Mass spectrometric analysis of B- $\Delta$ His<sub>3</sub>Asp following a denaturation protocol. The calculated and deconvoluted observed masses of S100A8(C42S)(H83A)(H87A) and biotinylated S100A9(H20A)(D30A) (-Met1) are shown. **(C)** CD spectra of 10  $\mu$ M B- $\Delta$ His<sub>3</sub>Asp in the absence and presence of Ca(II) in 1.0 mM Tris-HCl, pH 7.5. **(D)** Analytical SEC of 20  $\mu$ M B- $\Delta$ His<sub>3</sub>Asp in the absence and presence of 2 mM Ca(II) in 75 mM HEPES, 100 mM NaCl, pH 7.0. B- $\Delta$ His<sub>3</sub>Asp elutes at  $\approx$ 11.7 mL (-Ca(II)) and  $\approx$ 10.9 mL (+Ca(II)), and these peak elution volumes correspond to the  $\alpha\beta$  heterodimer and  $\alpha_2\beta_2$  heterotetramer, respectively.<sup>1</sup> **(E)** Zoom-in view of analytical SEC chromatograms presented in panel **D**. **(F)** Antimicrobial activity of  $\Delta$ His<sub>3</sub>Asp and B- $\Delta$ His<sub>3</sub>Asp against *E. coli* ATCC 25922. The mean OD<sub>600</sub> values and SEM are shown ( $n = 3$ ;  $t = 20$  h,  $T = 30$  °C, 150 rpm).

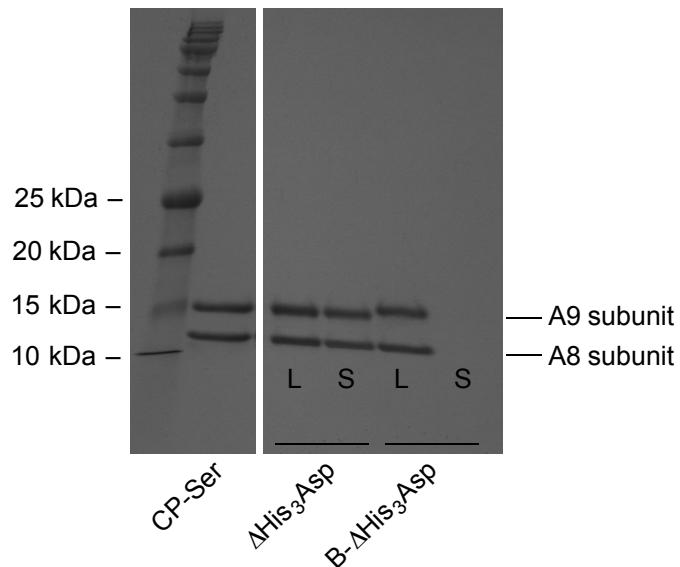


**Figure S6.** B-ΔHis<sub>3</sub>Asp binds to the streptavidin agarose resin. SDS-PAGE gel (15% Tris-glycine) of 10 μM ΔHis<sub>3</sub>Asp and B-ΔHis<sub>3</sub>Asp in 75 mM HEPES, 100 mM NaCl, pH 7.0 before (load, L) and after (supernatant, S) treatment with streptavidin agarose resin. The two panels are from the same gel. The lane adjacent to the ladder is a sample of 10 μM CP-Ser from another experiment.

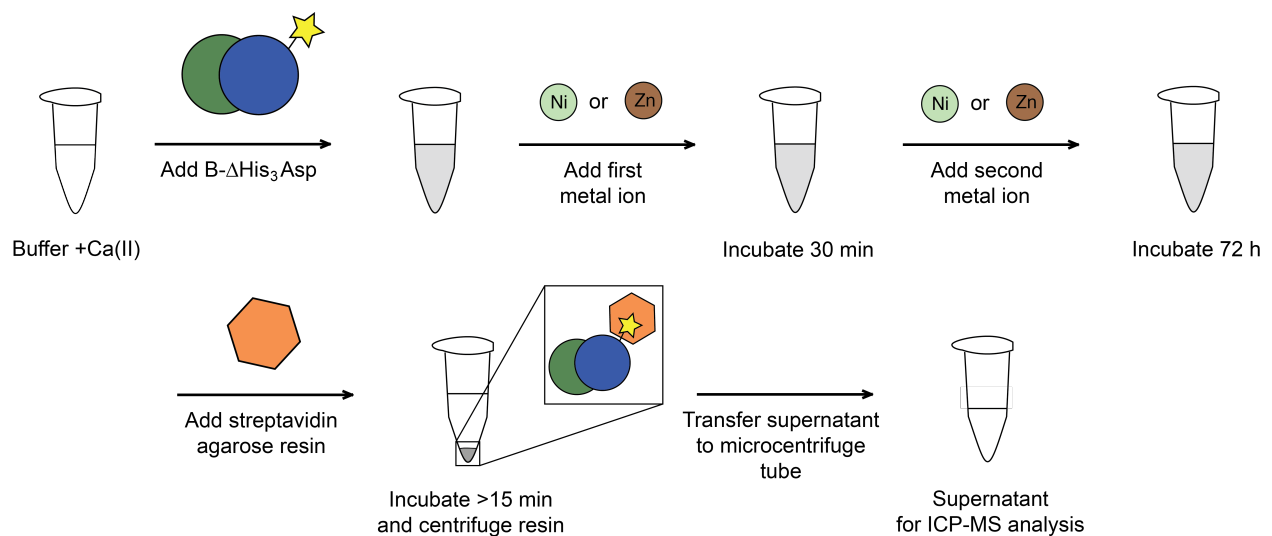


**Figure S7.** Schematic cartoon of the metal substitution assay. B-ΔHis<sub>3</sub>Asp was added to 75 mM HEPES, 100 mM NaCl, 2 mM CaCl<sub>2</sub>, pH 7.0. Mn(II), Fe(II), Ni(II), or Zn(II) was added to the protein solution and the mixture was equilibrated for 30 min at room temperature. A second metal was added, and the mixture was incubated for 72 h at 37 °C on an inverting platform. Streptavidin agarose resin was added, and the sample was incubated at room temperature for >15 min. The resin with streptavidin bound to biotinylated protein was pelleted by centrifugation (13,000 rpm, 3 min, 4 °C). The unbound metal content in the supernatant was measured by ICP-MS analysis.

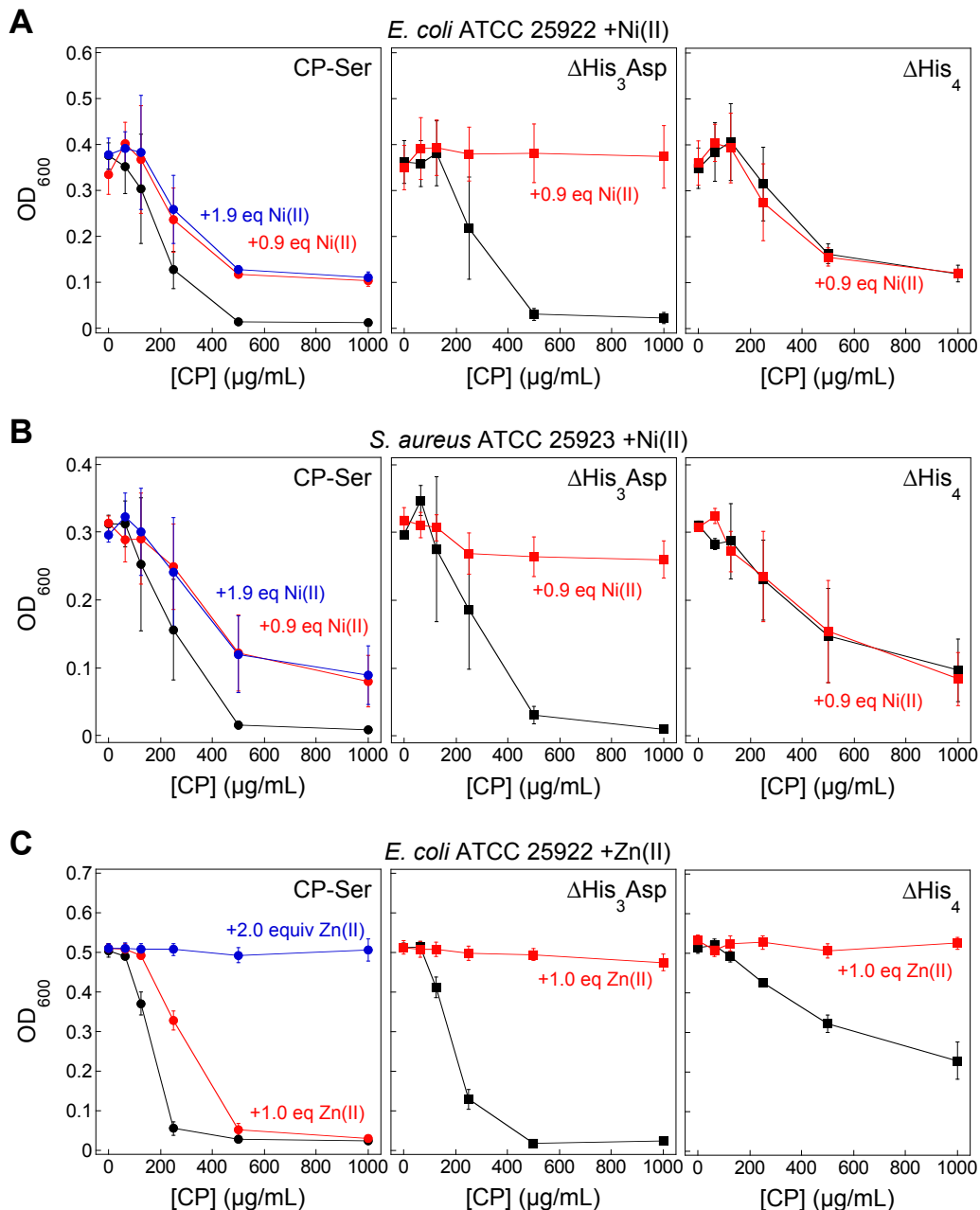


**Figure S8.** Metal preincubation attenuates the antimicrobial activity of CP-Ser. **(A)** Antibacterial activity of CP against *E. coli* ATCC 25922 with Ni(II) preincubation. **(B)** Antibacterial activity of CP-Ser against *S. aureus* ATCC 25923 with Ni(II) preincubation. **(C)** Antibacterial activity of CP-Ser against *E. coli* ATCC 25922 with Zn(II) preincubation. Bacteria were grown in the presence of CP-Ser (left),  $\Delta$ His<sub>3</sub>Asp (middle), and  $\Delta$ His<sub>4</sub> (right) in the absence (black lines) and presence of 1.0 equiv (red lines) or 2.0 equiv (blue lines) Ni(II) or Zn(II). The mean OD<sub>600</sub> values and SEM are reported ( $n = 3$ ,  $t = 20$  h,  $T = 30$  °C, 150 rpm).

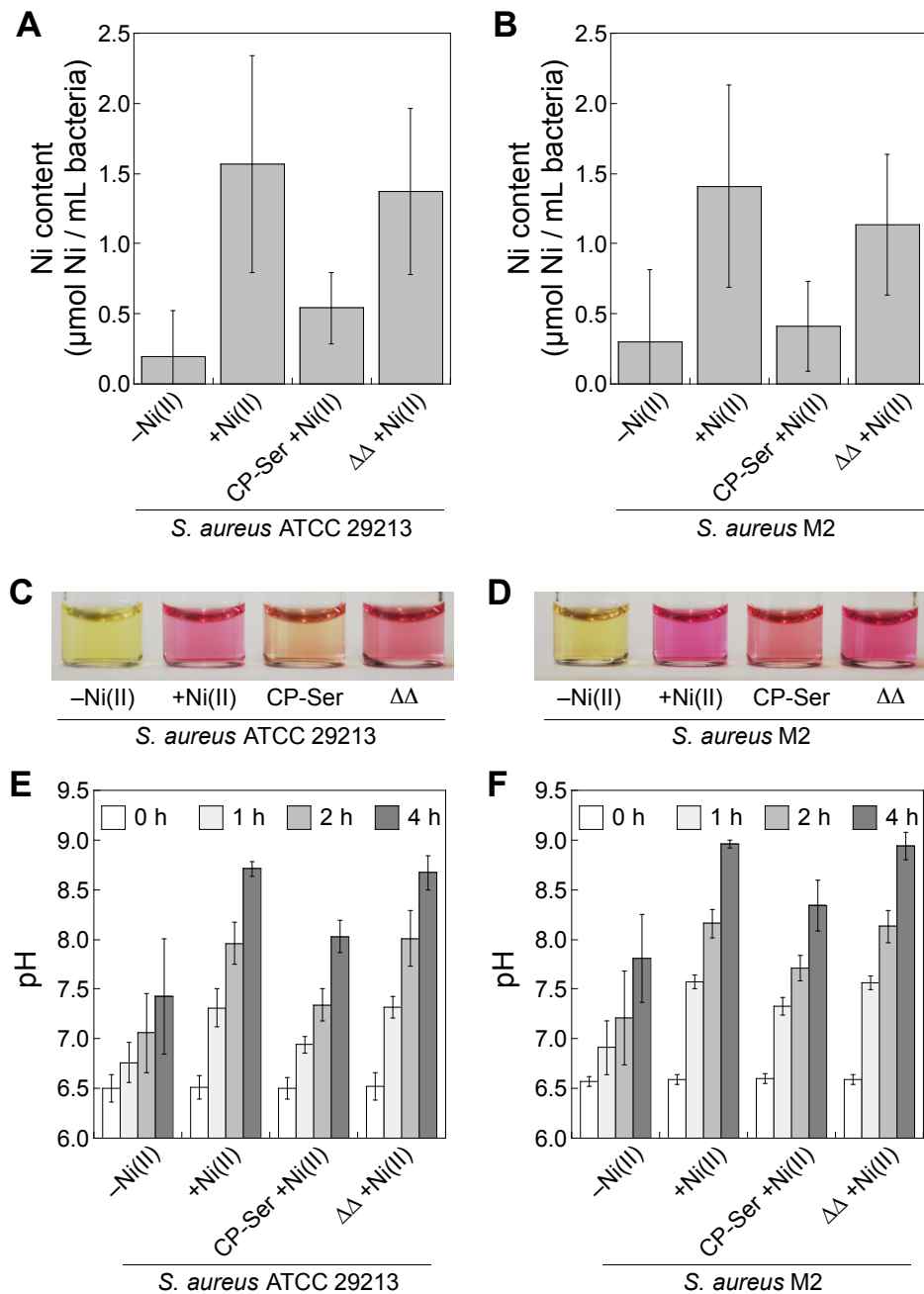


**Figure S9.** Ni(II) uptake assays and urease activity with *S. aureus* strains ATCC 29213 and *S. aureus* M2. (**A** and **B**) CP-Ser treatment results in decreased intracellular Ni as determined by ICP-MS. The mean Ni content of the bacterial suspensions ( $OD_{600} = 6$ ,  $\approx 10^9$  CFU/mL) and SDM are reported ( $n = 3$ ). (**C–F**) CP-Ser attenuates the urease activity of *S. aureus* ATCC 29213 and *S. aureus* M2 by CP as indicated by pH change. (**C** and **D**) Representative images of dCDMU supernatant incubated with bacteria treated with 1  $\mu$ M CP-Ser and  $\Delta\Delta$  in the presence of 1  $\mu$ M Ni(II) ( $t = 2$  h,  $T = 37$  °C). Phenol red turns from yellow to purple with increasing pH. The experiment was also conducted in the absence of Ni(II). (**E** and **F**) The pH was measured over the assay time course for each condition. The mean pH values and SDM are reported ( $n = 3$ ).

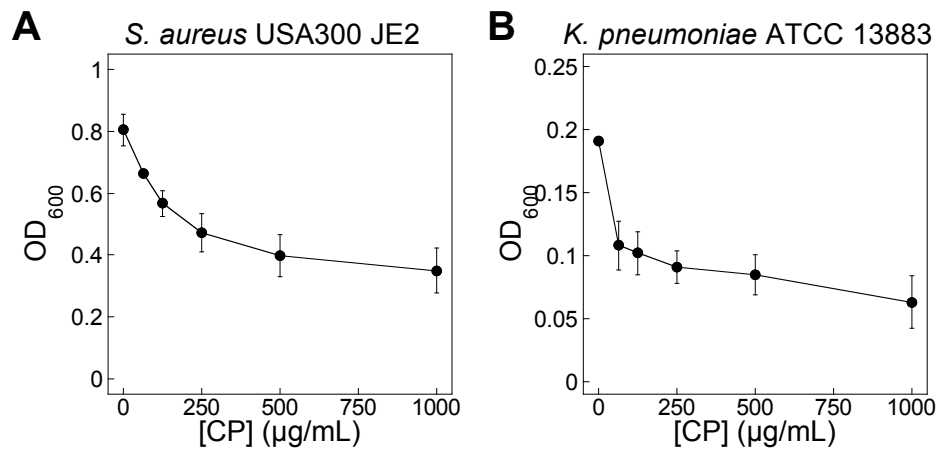


**Figure S10.** CP-Ser inhibits the growth of *S. aureus* and *K. pneumoniae* cultured in dCDM. Antibacterial activity of CP-Ser against **(A)** *S. aureus* and **(B)** *K. pneumoniae* grown in dCDM with 2 mM Ca(II). The OD<sub>600</sub> was measured at t = 20 h after incubation at T = 37 °C, 200 rpm. The mean OD<sub>600</sub> values and SEM are reported (n = 3).

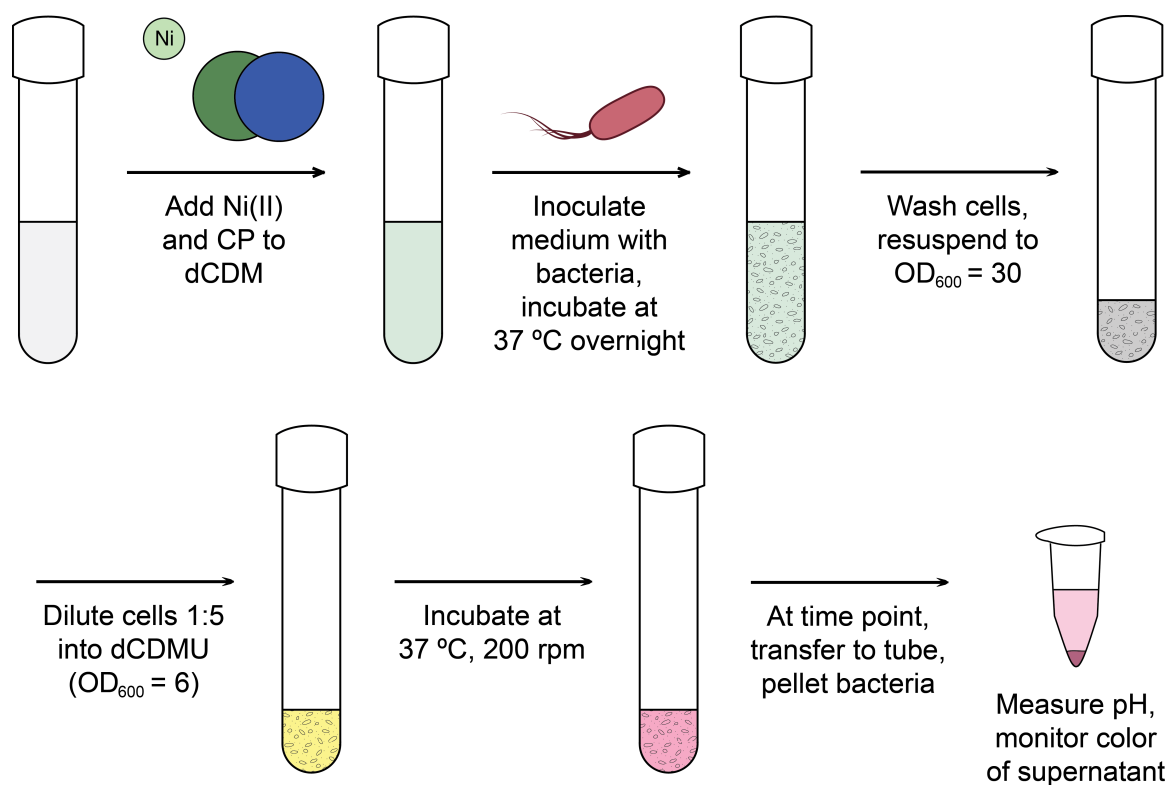


**Figure S11.** Schematic cartoon of the urease activity assay. A solution of dCDM was prepared with 1  $\mu\text{M}$  Ni(II) in the absence and presence of 1  $\mu\text{M}$  CP variant. An overnight culture of bacteria was inoculated into the medium (1:100 dilution). The cells were washed two or three times by centrifugation and resuspension in phosphate buffer (20 mM  $\text{NaH}_2\text{PO}_4$ , 100 mM NaCl, pH 6.8). After the final wash step, the cells were resuspended to an  $\text{OD}_{600} = 30$ . The bacterial suspension was diluted 1:5 into dCDMU ( $\text{OD}_{600} = 6$ ). At certain time points, a portion of the dCDMU bacterial suspension was transferred to a microcentrifuge tube and centrifuged to pellet the bacteria. The pH and color of the supernatant were monitored.

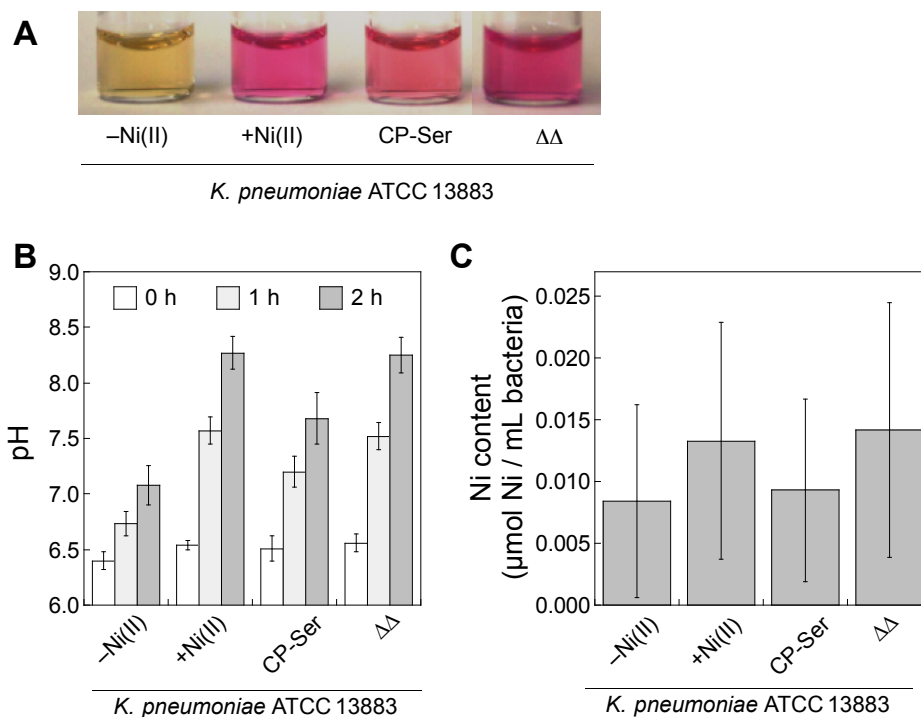


**Figure S12.** Urease activity and Ni(II) uptake assays with *K. pneumoniae* ATCC 13883. **(A)** CP-Ser attenuates the urease activity of *K. pneumoniae* ATCC 13883 as indicated by pH change. Representative images of dCDMU supernatant incubated with bacteria treated with 1 μM CP variants in the presence of 1 μM Ni(II) ( $t = 2$  h,  $T = 37$  °C). Phenol red turns from yellow to purple with increasing pH. The experiment was also conducted in the absence of Ni(II). **(B)** The pH was measured over the assay time course for each condition. The mean pH values and SDM are reported ( $n = 6$ ). **(C)** CP-Ser treatment results in decreased intracellular Ni as determined by ICP-MS. The mean Ni content of the bacterial suspensions ( $OD_{600} = 6$ ,  $\approx 10^9$  CFU/mL) and SDM are reported ( $n = 6$ ).



## Supporting References

- (1) Brophy, M. B.; Hayden, J. A.; Nolan, E. M. *J. Am. Chem. Soc.* **2012**, *134*, 18089–18100.
- (2) Brophy, M. B.; Nakashige, T. G.; Gaillard, A.; Nolan, E. M. *J. Am. Chem. Soc.* **2013**, *135*, 17804–17817.
- (3) Otwinowski, Z.; Minor, W. *Methods Enzymol.* **1997**, *276*, 307–326.
- (4) Morin, A.; Eisenbraun, B.; Key, J.; Sanschagrín, P. C.; Timony, M. A.; Ottaviano, M.; Sliz, P. *eLife* **2013**, *2*, e01456.
- (5) Gagnon, D. M.; Brophy, M. B.; Bowman, S. E. J.; Stich, T. A.; Drennan, C. L.; Britt, R. D.; Nolan, E. M. *J. Am. Chem. Soc.* **2015**, *137*, 3004–3016.
- (6) McCoy, A. J.; Grosse-Kunstleve, R. W.; Adams, P. D.; Winn, M. D.; Storoni, L. C.; Read, R. J. *J. Appl. Crystallogr.* **2007**, *40*, 658–674.
- (7) Adams, P. D.; Grosse-Kunstleve, R. W.; Hung, L.-W.; Ioerger, T. R.; McCoy, A. J.; Moriarty, N. W.; Read, R. J.; Sacchettini, J. C.; Sauter, N. K.; Terwilliger, T. C. *Acta Crystallogr. Sect. D: Biol. Crystallogr.* **2002**, *58*, 1948–1954.
- (8) Emsley, P.; Lohkamp, B.; Scott, W. G.; Cowtan, K. *Acta Crystallogr. Sect. D: Biol. Crystallogr.* **2010**, *66*, 486–501.
- (9) Taylor, D.; Holland, K. T. *J. Appl. Bacteriol.* **1989**, *66*, 319–329.
- (10) Fey, P. D.; Endres, J. L.; Yajjala, V. K.; Widhelm, T. J.; Boissy, R. J.; Bose, J. L.; Bales, K. W. *mBio* **2013**, *4*, e00537-e005312.
- (11) Harro, J. M.; Daugherty, S.; Bruno, V. M.; Jabra-Rizk, M. A.; Rasko, D. A.; Shirliff, M. E. *Genome Announc.* **2013**, *1*, e00037-00012.
- (12) Nguyen, A. T.; Jones, J. W.; Ruge, M. A.; Kane, M. A.; Oglesby-Sherrouse, A. G. *J. Bacteriol.* **2015**, *197*, 2265–2275.
- (13) Robert-Baldo, G. L.; Morris, M. J.; Byrne, R. H. *Anal. Chem.* **1985**, *57*, 2564–2567.
- (14) Weatherburn, M. W. *Anal. Chem.* **1967**, *39*, 971–974.

- (15) Damo, S. M.; Kehl-Fie, T. E.; Sugitani, N.; Holt, M. E.; Rathi, S.; Murphy, W. J.; Zhang, Y.; Betz, C.; Hench, L.; Fritz, G.; Skaar, E. P.; Chazin, W. J., *Proc. Natl. Acad. Sci. U.S.A.* **2013**, *110*, 3841–3846.
- (16) Lebrette, H.; Borezee-Durant, E.; Martin, L.; Richaud, P.; Boeri Erba, E.; Cavazza, C. *Metallomics* **2015**, *7*, 613–621.
- (17) Ermler, U.; Grabarse, W.; Shima, S.; Goubeaud, M.; Thauer, R. K. *Science* **1997**, *278*, 1457–1462.
- (18) Pochapsky, T. C.; Pochapsky, S. S.; Ju, T.; Hoefler, C.; Liang, J. *J. Biomol. NMR* **2006**, *34*, 117–127.
- (19) He, M. M.; Clugston, S. L.; Honek, J. F.; Matthews, B. W. *Biochemistry* **2000**, *39*, 8719–8727.
- (20) Pearson, M. A.; Michel, L. O.; Hausinger, R. P.; Karplus, P. A. *Biochemistry* **1997**, *36*, 8164–8172.
- (21) Shi, R.; Munger, C.; Asinas, A.; Benoit, S. L.; Miller, E.; Matte, A.; Maier, R. J.; Cygler, M. *Biochemistry* **2010**, *49*, 7080–7088.
- (22) Barondeau, D. P.; Kassmann, C. J.; Bruns, C. K.; Tainer, J. A.; Getzoff, E. D. *Biochemistry* **2004**, *43*, 8038–8047.
- (23) Volbeda, A.; Martin, L.; Cavazza, C.; Matho, M.; Faber, B. W.; Roseboom, W.; Albracht, S. P. J.; Garcin, E.; Rousset, M.; Fontecilla-Camps, J. C. *J. Biol. Inorg. Chem.* **2005**, *10*, 239–249.
- (24) Schreiter, E. R.; Wang, S. C.; Zamble, D. B.; Drennan, C. L. *Proc. Natl. Acad. Sci. U.S.A.* **2006**, *103*, 13676–13681.
- (25) Desguin, B.; Zhang, T.; Soumillion, P.; Hols, P.; Hu, J.; Hausinger, R. P. *Science* **2015**, *349*, 66–69.
- (26) Yu, Y.; Zhou, M.; Kirsch, F.; Xu, C.; Zhang, L.; Wang, Y.; Jiang, Z.; Wang, N.; Li, J.; Eitinger, T.; Yang, M. *Cell Res.* **2014**, *24*, 267–277.

- (27) Smith, R. M.; Martell, A. E. *Critical Stability Constants Volume 2: Amines*; Plenum Press: New York, 1975; Vol. 2.
- (28) Smith, R. M.; Martell, A. E. *Critical Stability Constants*; Springer Science+Business Media: New York, 1975; Vol. 6.
- (29) Smith, R. M.; Martell, A. E. *Critical Stability Constants*; Springer Science+Business Media: New York, 1982; Vol. 5.